



CENTRE DE RECERCA MATEMÀTICA

This is a preprint of: *Stochastic quasi-steady state approximations for asymptotic solutions of the Chemical Master Equation*

Journal Information: *J. Chem. Phys.*,

Author(s): T. Alarcon.

Volume, pages: 140(18) 1-18, DOI:[doi.org/10.1063/1.4874653]

Stochastic quasi-steady state approximations for asymptotic solutions of the chemical master equation

Cite as: J. Chem. Phys. **140**, 184109 (2014); <https://doi.org/10.1063/1.4874653>

Submitted: 20 December 2013 . Accepted: 22 April 2014 . Published Online: 12 May 2014

Tomás Alarcón



View Online



Export Citation



CrossMark

ARTICLES YOU MAY BE INTERESTED IN

[Stochastic chemical kinetics and the quasi-steady-state assumption: Application to the Gillespie algorithm](#)

The Journal of Chemical Physics **118**, 4999 (2003); <https://doi.org/10.1063/1.1545446>

[The chemical Langevin equation](#)

The Journal of Chemical Physics **113**, 297 (2000); <https://doi.org/10.1063/1.481811>

[The Relationship between Stochastic and Deterministic Models for Chemical Reactions](#)

The Journal of Chemical Physics **57**, 2976 (1972); <https://doi.org/10.1063/1.1678692>

The Journal
of Chemical Physics

Submit Today

The Emerging Investigators Special Collection and Awards
Recognizing the excellent work of early career researchers!

Stochastic quasi-steady state approximations for asymptotic solutions of the chemical master equation

Tomás Alarcón^{1,2}

¹*Centre de Recerca Matemàtica, Edifici C, Campus de Bellaterra, 08193 Bellaterra (Barcelona), Spain*

²*Departament de Matemàtiques, Universitat Autònoma de Barcelona, 08193 Bellaterra (Barcelona), Spain*

(Received 20 December 2013; accepted 22 April 2014; published online 12 May 2014)

In this paper, we propose two methods to carry out the quasi-steady state approximation in stochastic models of enzyme catalytic regulation, based on WKB asymptotics of the chemical master equation or of the corresponding partial differential equation for the generating function. The first of the methods we propose involves the development of multiscale generalisation of a WKB approximation of the solution of the master equation, where the separation of time scales is made explicit which allows us to apply the quasi-steady state approximation in a straightforward manner. To the lowest order, the multi-scale WKB method provides a quasi-steady state, Gaussian approximation of the probability distribution. The second method is based on the Hamilton-Jacobi representation of the stochastic process where, as predicted by large deviation theory, the solution of the partial differential equation for the corresponding characteristic function is given in terms of an effective action functional. The optimal transition paths between two states are then given by those paths that maximise the effective action. Such paths are the solutions of the Hamilton equations for the Hamiltonian associated to the effective action functional. The quasi-steady state approximation is applied to the Hamilton equations thus providing an approximation to the optimal transition paths and the transition time between two states. Using this approximation we predict that, unlike the mean-field quasi-steady approximation result, the rate of enzyme catalysis depends explicitly on the initial number of enzyme molecules. The accuracy and validity of our approximated results as well as that of our predictions regarding the behaviour of the stochastic enzyme catalytic models are verified by direct simulation of the stochastic model using Gillespie stochastic simulation algorithm. © 2014 AIP Publishing LLC. [<http://dx.doi.org/10.1063/1.4874653>]

I. INTRODUCTION

The Michaelis-Menten (MM) model for enzyme kinetics and its mathematical analysis by means of the quasi-steady (QSS) approximation are two cornerstones of mathematical modelling in biochemistry. The MM model was originally proposed to explain the departure of the rate of the enzymatic reaction from the one obtained by direct application of the law of mass action.¹ It was observed that the speed of transformation of substrate into product as a function of substrate concentration has an upper bound. In order to explain this behaviour, the model schematically represented in Fig. 1 was proposed. The enzyme-mediated transformation of the substrate (S) into the product (P) is described as a two-step process involving the formation of an intermediate complex (C) which eventually decays into the product and the enzyme molecules.

Originally, the mathematical description of the reaction mechanism shown in Fig. 1 consisted of three ordinary differential equations (ODEs). In order to simplify this system and obtain analytical expressions for the speed of the reaction, several approximations were proposed. In their original paper, Michaelis and Menten² assumed that the substrate is in equilibrium with the complex. This assumption allows to eliminate one of the variables and express the rate of product formation as a function of substrate concentration. Later on, Briggs and Haldane³ introduced an alternative approximation

where they assumed that the rates of formation and decay of the complex were very similar, so that the amount of complex should remain approximately constant. Mathematically,¹ it can be shown that this can be achieved by assuming that the total amount of enzyme, e_0 , and the characteristic scale for the amount of substrate, s_0 , satisfy $e_0 \ll s_0$. When this condition is satisfied, the quasi-steady-state approximation can be invoked.¹ In either case, this type of approximation relies on a separation of time scales. In the case of the MM model for enzyme catalysis, the assumption is that the dynamics of the formation of the complex is much faster than that of the substrate and the product. In the remainder of this paper, we focus on the regime of low enzyme concentration.

In spite of the many applications found over the years for both the MM model for enzyme kinetics and its QSS approximation,¹ serious limitations have been uncovered, specially in *in vivo* situations. Generally speaking, the physical rationale for the standard mathematical treatment of the MM model shown in Fig. 1, i.e., mean-field, ordinary differential equations for the time evolution of the concentration of each chemical species, is based on two assumptions, namely, the reactions occur in a well-mixed, impurity-free environment, and the number of molecules is big enough for random effects to be negligible. These conditions are far from the ones encountered in *in vivo* systems. The cellular environment in which enzymatic reactions take place is highly inhomogeneous and crowded with macromolecules.^{4,5}

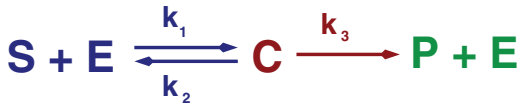


FIG. 1. Schematic representation of the Michaelis-Menten model of enzymatic catalysis: A substrate, S , which is stable in the absence of the enzyme E , forms a complex, C , with the enzyme. The complex eventually decays into a product, P , and the unmodified enzyme.

Furthermore, in such *in vivo* situations, the number of molecules participating in enzyme-catalytic reactions, is small, whereby noise may become a dominant factor.^{6–8} Several approaches have been proposed to deal with these issues. For example, regarding the effects of inhomogeneities and molecular crowding in intracellular environments, models invoking the use of fractal-like kinetics have been proposed^{4,5,9} to improve upon standard law-of-mass-action kinetics. Similarly, the issue of the noise-induced breakdown of the mean-field approximation has been extensively studied^{6–8} and several stochastic models have been proposed to deal with systems where low number of molecules are considered.

Our aim in this paper is to formulate stochastic generalisations of the QSS approximation for enzyme-catalysed reactions. We will focus on noise effects due to low number of molecules, leaving aside for the time being the effects of the intracellular environment. Our analysis takes place in the context of Markovian models of the reaction mechanism shown in Fig. 1 formulated in terms of the so-called chemical master equation (CME).¹⁰ We will formulate QSS approximations for asymptotic solutions of the CME obtained by means of large deviations/WKB approximations^{11,12} in the low enzyme concentration regime. The CME is given:

$$\frac{\partial P(x, t)}{\partial t} = \sum_i W_i(x - r_i)P(x - r_i, t) - W_i(x)P(x, t), \quad (1)$$

where $W_i(x)$ is the transition rate corresponding to reaction channel i and r_i is a vector whose entries are the increase in the number of molecules of each molecular species when reaction channel i fires up, i.e., $P(x(t + \Delta t) = x(t) + r_i | x(t)) = W_i(x)\Delta t$. The transition rates corresponding to the enzymatic reaction Fig. 1 are given in Table I.

There are several precedents of approximations which attempt to take advantage of the separation of time scales in stochastic models of enzyme catalysis. Several such analyses have been carried out in which the equilibrium approximation is applied directly to the master equation (Eq. (1)) by

setting the fast reactions in stochastic partial equilibrium (i.e., the probability distribution corresponding to the fast variables remains unchanged), and letting the rest of the system to evolve according to a reduced stochastic dynamics.^{13,14} Other approaches consist of applying a quasi-steady state approximation to the exact Fokker-Planck equation that can be derived from the Poisson representation of the chemical master equation.¹⁵ Approaches based enumeration techniques have also been proposed.¹⁶ Furthermore, Thomas *et al.*¹⁷ have recently formulated a rigorous method to eliminate fast stochastic variables in monostable systems using projector operators within the linear noise approximation.¹⁷ In addition, there has also been much activity in recent years regarding the development of numerical methods for stochastic systems with multiple time scales.^{18–20} Several of these methods are modifications of the standard Gillespie stochastic simulation algorithm^{13,21–25} or the τ -leap method²⁶ where the existence of fast and slow variables allows to improve efficiency with respect to the standard algorithms by means of the stochastic partial equilibrium assumption. Another family of numerical methods which exploit the presence of fast and slow processes to increase efficiency is that of the so-called hybrid methods, where classical deterministic rate equations or stochastic Langevin equations for the fast variables are combined with the classical stochastic simulation algorithm for the slow variables.^{27,28}

In this paper, we use two different approaches to formulate stochastic versions of the quasi-steady state approximation, both based on WKB asymptotics of either the solution of Master Equation^{11,29} or the solution of the partial differential equation (PDE) satisfied by the corresponding generating function.³⁰ First, we develop a QSS approximation based on a multi-scale WKB solution of the chemical master equation, which is a generalisation of the WKB solution of the master equation first introduced by Kubo *et al.*^{11,29,31} We then proceed to develop a second stochastic QSS approximation, which allows us to find the optimal transition paths between two states, which can be extended to compute transition paths between stable states in bistable systems whose dynamic is described by Eq. (1). These transition paths are determined as the solutions of an optimisation problem for an effective action functional which, according to the theory of large deviations,^{12,30,32} determines the solution of the partial differential equation for the generating function associated to the probability distribution corresponding to Eq. (1). The optimisation problem takes the form of a set of Hamilton equations for the Hamiltonian associated to the effective action functional. These two approximations have different scopes: whereas the multi-scale WKB QSSA provides a Gaussian approximation to the full probability distribution, the Hamilton-Jacobi QSSA allows us to study large fluctuations and rare events by computing the optimal fluctuation paths and the average transition times associated to these rare events.

The remainder of this paper is organised as follows. In Sec. II, we develop a multi-scale extension of the WKB approximation developed by Kubo *et al.*¹¹ and its application to the quasi-steady state approximation for the basic enzymatic reaction shown in Fig. 1. In Sec. III, we introduce the quasi-steady approximation in the context of the Hamilton-Jacobi

TABLE I. Transition rates corresponding to the enzymatic reaction schematically represented in Fig. 1. Product molecules (denoted as P in Fig. 1) are not considered.

Transition rate	r	Event
$W_1(x) = k_1 x_1 x_2$	$r_1 = (-1, -1, +1)$	Enzyme and substrate form complex
$W_2(x) = k_2 x_3$	$r_2 = (+1, +1, -1)$	Complex splits into its components
$W_3(x) = k_3 x_3$	$r_3 = (0, +1, -1)$	Complex produces product and liberates enzyme

representation of the corresponding stochastic process. This method is applied to the enzymatic reaction shown in Fig. 1 as well as to an enzymatic activation/inactivation system which exhibits mutual inhibition and bistability. We show that this method allows us to compute optimal fluctuation paths. We also show that, unlike the deterministic QSSA, the stochastic QSSA is such that the rate of enzymatic (in)activation exhibits explicit dependence on the initial number of enzyme molecules. Finally, in Sec. IV, we discuss our results as well as open questions for future research.

II. MULTI-SCALE WKB METHOD

In this section, we present an asymptotic method based on the WKB approximation for the CME first introduced by Kubo *et al.*,¹¹ complemented with recent developments on asymptotic analysis of multi-scale reaction networks.³¹ This method, which we refer to as the multi-scale WKB (MSWKB) approximation, is based on the assumption that both species abundance and the corresponding rate constants scale in a certain way with a parameter, Ω .³¹ The scaling parameter does not represent the size of the model in terms of volume or Avogadro's number as in the classical WKB approximation:¹¹ Its physical meaning will vary between different models but it will have a specific (large) value in any physical or biological problem.³¹

Following Ball *et al.*,³¹ we assume that each state variable of our system, x_i , can be expressed in terms of a scaled variable, z_j , such that:

$$z_j = \Omega^{-\alpha_j} x_j, \quad (2)$$

where $\alpha_j > 0$. We further assume that, as a result of Eq. (2), the transition rates, $W_i(x)$, scale with Ω so that the following scaling relation

$$W_i(x) = \Omega^{\beta_i - \alpha_0} w_i(z) \quad (3)$$

is satisfied. Consequently, the CME (Eq. (1)) can be re-written as

$$\frac{1}{\Omega^{\alpha_0}} \frac{\partial P(z, t)}{\partial t} = \sum_i \Omega^{\beta_i - \alpha_0} (w_i(z - y_i) P(z - y_i, t) - w_i(z) P(z, t)), \quad (4)$$

where $\alpha_0 = \min_j \alpha_j$, $y_i = (y_{i,j})$ with $y_{i,j} = \Omega^{-\alpha_j} r_{i,j}$. To proceed further, we consider the characteristic function of $P(z, t)$,

$$Q(u, t) = \int_{-\infty}^{\infty} P(z, t) e^{iu \cdot z} dz, \quad (5)$$

and its associated cumulant generating function $q(u, t) \equiv \log(Q(u, t))$,^{11,29} as the cumulants $q_n(t)$ of $P(z, t)$ can be obtained from the expansion:

$$q(u, t) = \sum_{n=1}^{\infty} \frac{i^n}{n!} u^n \cdot q_n(t), \quad (6)$$

where u^n stands for the n -adic product defined as $(u^n)_{j_1, j_2, \dots, j_n} \equiv \prod_{i=1}^n u_{j_i}$ and “ \cdot ” denotes full contraction over all of the n indexes. It can be shown²⁹ that, in terms of the

characteristic function $Q(u, t)$, Eq. (4) is given by

$$\frac{1}{\Omega^{\alpha_0}} \frac{\partial Q(u, t)}{\partial t} = \frac{1}{(2\pi)^d} \sum_i (e^{-iu \cdot y_i} - 1) \times \int_{-\infty}^{\infty} \Omega^{\beta_i - \alpha_0} w_i(v) Q(u - v, t) dv, \quad (7)$$

where $w_i(v)$ is the Fourier transform of $w_i(z)$ as defined in Eq. (3). Kubo *et al.*¹¹ showed that Eq. (7) is the starting point for an asymptotic expansion of the WKB type, where a closed hierarchy of ordinary differential equations for the cumulants ($q_n(t)$) of the process is obtained. In Appendix A, we show how this asymptotic method can be extended to multi-scale situations where different variables scale differently with Ω , a situation which had not been considered before in the context of this method. To the lowest order, as derived in Appendix A, the stochastic QSS approximation according to the MSWKB method is given by

$$\begin{aligned} \sum_i r_{i,j} v_i(s) &= 0 \text{ if } j \neq j_1 \\ \sum_i 2 \sum_l \left(r_{i,j} S_{jl} \frac{\partial v_i(s)}{\partial s_l} + r_{i,j_1} S_{jl} \frac{\partial v_i(s)}{\partial s_l} \right) &+ \sum_i r_{i,j} r_{i,j_1} v_i(s) = 0 \text{ if } j, k \neq j_1, \end{aligned} \quad (8)$$

where $\alpha_1 = \max_j \alpha_j$ and j_1 be such that $\alpha_{j_1} = \alpha_1$ and $v_i(s)$ is the inverse Fourier transform of $\Omega^{\beta_i - \alpha_0 - \alpha_1} w_i(v)$ (see Appendix A), and

$$\begin{aligned} \frac{ds_{j_1}}{d\tau} &= \sum_i r_{i,j} v_i(s) \\ \frac{dS_{jj_1}}{d\tau} &= \sum_i 2 \sum_l \left(r_{i,j} S_{jl} \frac{\partial v_i(s)}{\partial s_l} + r_{i,j_1} S_{jl} \frac{\partial v_i(s)}{\partial s_l} \right) \\ &+ \sum_i r_{i,j} r_{i,j_1} v_i(s), \end{aligned} \quad (9)$$

with $\Omega^{-\alpha_k} S_{kj} = \Omega^{-\alpha_j} S_{jk}$. As shown in Appendix A, s_j corresponds to the lowest order approximation of components of the first cumulant, and the matrix elements S_{jk} correspond to the lowest order approximation of the re-scaled elements of second cumulant, i.e., the entries of the covariance matrix. Equation (8) provides $s_j(s_{j_1})$ and $S_{jk}(s_{j_1}, S_{j,j_1}, S_{j_1,k})$ which are then used to solve Eq. (9).

The probabilistic expression of the quasi-steady state approximation takes the form:

$$P(z) = P_{QSS}(z_1, \dots, z_{j_1-1} | z_{j_1}) P_{j_1}(z_{j_1}), \quad (10)$$

where we have re-ordered the components of the vector z so that $j_1 = d$. Consistent with our calculation, where we have obtained the leading order approximation for the first two cumulants of the probability distribution function, we approximate P_{QSS} and P_{j_1} by Gaussian distributions:

$$\begin{aligned} P_{j_1}(z_{j_1}) &= \frac{\Omega^{\alpha_1/2}}{\sqrt{2\pi}\sigma} e^{-\frac{\Omega^{\alpha_1}(z_{j_1}-s_{j_1})^2}{2\sigma^2}}, \\ P_{QSS}(z | z_{j_1}) &= \frac{1}{\sqrt{2\pi} \det(\mathcal{S})} e^{-\Omega^{\alpha_1}(z-p)^T \cdot \mathcal{S}^{-1} \cdot (z-p)}, \end{aligned} \quad (11)$$

where we have defined $\sigma = S_{j_1 j_1}$, $z = (z_j)$ with $j = 1, \dots, j_1 - 1$, $p = (s_j)$ with $j = 1, \dots, j_1 - 1$, and $\mathcal{S} = (\Omega^{\alpha_1 - \alpha_j} S_{ij})$ with $j, k = 1, \dots, j_1 - 1$.

A. Particular case: The Michaelis-Menten model of enzyme kinetics

As an example of the MSWKB method, we now focus on the archetypal application of the quasi-steady state approximation, namely, the stochastic version of the Michaelis-Menten model of enzyme kinetics,¹ schematically depicted in Fig. 1. We will use the parameter values provided in Ref. 13.

According to the chemical kinetics defined by the transition rates prescribed in Table I and according to Eqs. (8) and (9), we have the following equations for the first cumulant, i.e., the mean-field equations:

$$\begin{aligned} \frac{ds_1}{d\tau} &= -k_1 s_1 s_2 + \kappa_2 s_3, \\ -k_1 s_1 s_2 + (\kappa_2 + \kappa_3) s_3 &= 0, \\ k_1 s_1 s_2 - (\kappa_2 + \kappa_3) s_3 &= 0, \end{aligned} \quad (12)$$

where $s_1(t) = \langle x_1(t) \rangle$, $s_2(t) = \langle x_2(t) \rangle$, and $s_3(t) = \langle x_3(t) \rangle$, i.e., the average concentrations of substrate, enzyme, and complex, respectively, and $\kappa_2 = \Omega^{-1} k_2$ and $\kappa_3 = \Omega^{-1} k_3$. Note that the last two equations are not linearly independent. This is a direct consequence of the conservation of the total amount enzyme (free plus forming a complex with a substrate molecule): $s_2 + s_3 = 1$. Taken together, Eq. (12) and the conservation law imply that

$$\frac{ds_1}{d\tau} = -\frac{k_1 \kappa_3}{\kappa_2 + \kappa_3 + k_1 s_1} s_1, \quad (13)$$

$$s_3 = \frac{k_1 s_1}{(\kappa_2 + \kappa_3 + k_1 s_1)}. \quad (14)$$

The stochastic QSS approximation is completed by the solution of corresponding system of differential-algebraic equations (DAEs) for the entries of re-scaled covariance matrix, S_{jk} . As shown in Appendix A, the quantities S_{jk} satisfy $S_{13} = \epsilon S_{31}$. Taking this into account, the system of DAEs for the quantities S_{jk} are given by

$$\frac{dS_{11}}{d\tau} = -4k_1(1 - s_3)S_{11} + \frac{(2\kappa_2 + \kappa_3)k_1 s_1}{(\kappa_2 + \kappa_3 + k_1 s_1)}, \quad (15)$$

$$\begin{aligned} \frac{dS_{31}}{d\tau} &= 2(-k_1(1 - 2s_3)S_{31} + k_1(1 - s_3)S_{11} \\ &\quad - (k_1 s_1 + \kappa_2)S_{33}) - \frac{(2\kappa_2 + \kappa_3)k_1 s_1}{(\kappa_2 + \kappa_3 + k_1 s_1)}, \end{aligned} \quad (16)$$

$$\begin{aligned} 0 &= 4(k_1(1 - s_3)S_{31} - (k_1 s_1 + \kappa_2 + \kappa_3)S_{33}) \\ &\quad + 2\frac{(\kappa_2 + \kappa_3)k_1 s_1}{\kappa_2 + \kappa_3 + k_1 s_1}. \end{aligned} \quad (17)$$

Note that we have applied the MSWKB method to a reduced two-variable, x_1 and x_3 . All the relevant statistical information about the third random variable, x_2 , can be retrieved from the relation $x_2 + x_3 = e_0$ and the knowledge of the conditional probability distribution function $P(x_3|x_1)$ given by Eq. (11). The system of DAEs (Eqs. (13)–(17)) has been solved using Matlab's implicit solver `ode15s`. The corresponding results are shown in Figs. 2(a) and 2(b).

In order to assess the accuracy of our MSWKB approximation, we have run simulations of the stochastic enzyme kinetics model (see Table I) and compared the results to our asymptotic results Eqs. (11) and (13)–(17). Our results are shown in Fig. 3(a), where we show realisations of stochastic enzyme kinetics model generated using the stochastic simulation algorithm (SSA),³³ in particular, we show the stochastic time evolution of the number of substrate molecules, $x_1(t)$. The Gaussian approximation Eq. (11) implies that a 68.2% of the realisations should stay within the region delimited by the

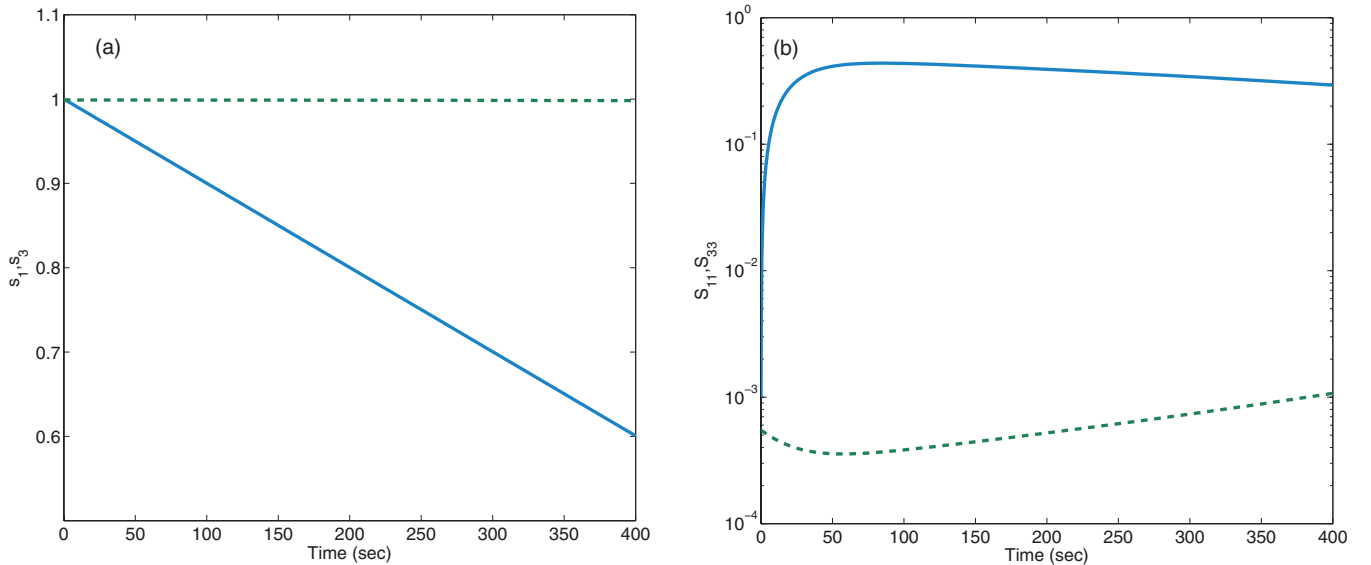


FIG. 2. Numerical solution of the MSWKB approximation for the Michaelis-Menten model Eqs. (13)–(17). Plot (a) shows results for the average concentration of substrate (blue solid line), s_1 , and complex (green dashed line), s_3 , whereas plot (b) shows results for the diagonal elements of the covariance matrix associated to the substrate, S_{11} , (solid blue line) and to the complex, S_{33} , (dashed green line). Parameter values: $\Omega = 10^3$, $k_1 = k_2 = 1 \text{ s}^{-1}$, $k_3 = 0.1 \text{ s}^{-1}$, $\alpha_1 = 1$, and $\alpha_2 = \alpha_3 = 1/3$.¹³

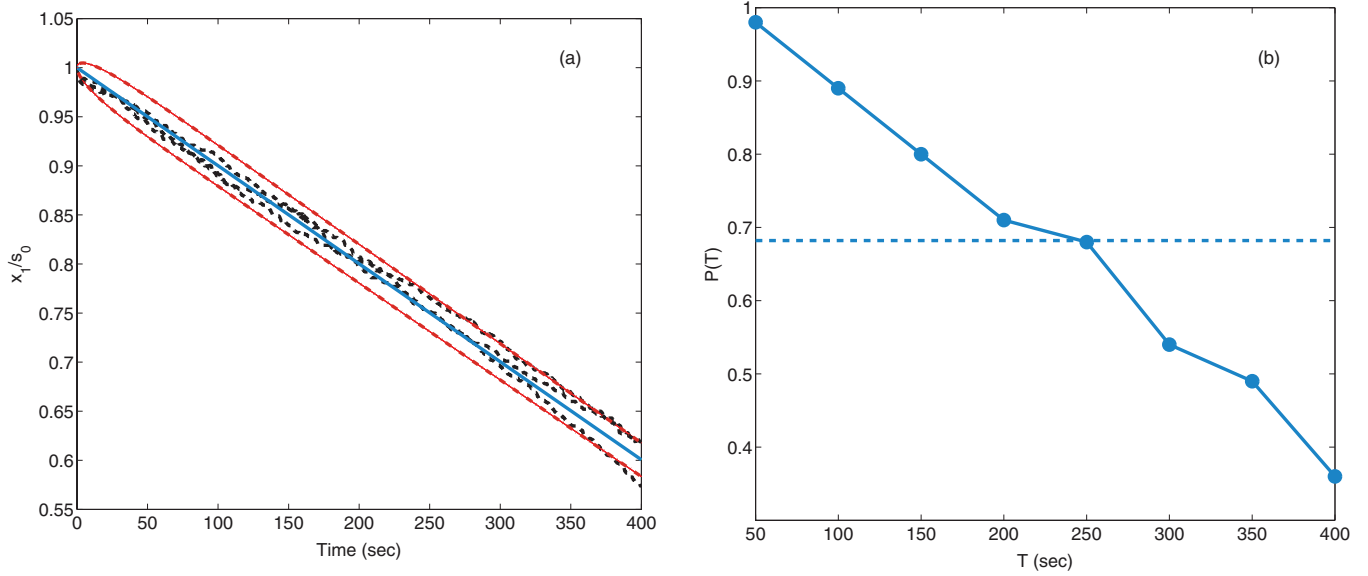


FIG. 3. Colour code for panel (a): Solid blue line represents $s_1(\tau)$ as given by the system of DAEs (Eqs. (13)–(17)), red dashed-dotted lines correspond to $s_1(\tau) \pm \Omega^{-\alpha_0/2}\sigma(\tau)$ (see Eq. (11)), and black dashed lines correspond to direct simulation of the stochastic process described in Table I where we show the time evolution of x_1/Ω^{α_0} . Panel (b): Average over 1000 realisations. Parameter values (both figures): $\Omega = 10^3$, $k_1 = k_2 = 1 \text{ s}^{-1}$, $k_3 = 0.1 \text{ s}^{-1}$, $\alpha_1 = 1$, and $\alpha_2 = \alpha_3 = 1/3$.¹³

upper and lower boundaries given by $s_1(\tau) \pm \Omega^{-\alpha_0/2}\sigma(\tau)$, respectively, where $\sigma(\tau) = \sqrt{S_{11}(\tau)}$. Our asymptotic result appears to capture the behaviour of the actual stochastic system with accuracy: Only for longer times when $x_1 \ll \Omega^{\alpha_0}$ the approximation appears to break down (as indicated by the fact that the corresponding sample path for x_1 crosses either of the boundaries $s_1(\tau) \pm \Omega^{-\alpha_0/2}\sigma(\tau)$). The reason for this is that for longer times, we observe that $x_1 \ll \Omega^{\alpha_0}$ and therefore the scaling hypothesis implicit in our MSWKB Ansatz,^{10,11} $x_1 \sim \Omega^{\alpha_0}$, is no longer valid. For earlier times, our scaling hypothesis holds and our asymptotic approximation provides an accurate description of the behaviour of the system. This is further quantified in Fig. 3(b) which shows the probability of a realisation of the process to be within these boundaries for all time $\tau \leq T$ as a function of T , $P(T)$. In order for our Gaussian approximation to be valid, 68.2% of the realisations should stay within the region delimited by the upper and lower boundaries given by $s_1(\tau) \pm \Omega^{-\alpha_0/2}\sigma(\tau)$, i.e., $P(T) \geq 0.682$. Results shown in Fig. 3(b) imply that such condition is satisfied for shorter times. For longer times x_1 becomes too small for our two fundamental hypothesis involved in obtaining the stochastic QSSA to hold. The WKB Ansatz for CME requires the number of substrate molecules to be large. Similarly, the validity of QSS approximation is based on the assumption that the number of substrate molecules is much larger than the number of enzyme molecules. Thus, as time progresses and x_1 decreases, our two hypotheses cease to be valid.

III. QUASI-STEADY STATE APPROXIMATION IN THE HAMILTON-JACOBI REPRESENTATION

An alternative way to analyse the dynamics of continuous-time Markov processes on a discrete space of states is to derive an equation for the generating function,

$G(p_1, \dots, p_n, t)$ of the corresponding probabilistic density:

$$G(p_1, \dots, p_n, t) = \sum_x p_1^{x_1} p_2^{x_2} \cdots p_n^{x_n} P(x_1, \dots, x_n, t), \quad (18)$$

where $P(x_1, \dots, x_n, t)$ is the solution of the Master Equation (1). $G(p_1, \dots, p_n, t)$ satisfies a partial differential equation which can be derived from the Master Equation. This PDE is the basic element of the so-called momentum representation of the Master Equation.³² The corresponding PDE can be solved explicitly only in a few simple cases. However, although closed, analytic solutions are rarely available the PDE for the generating function admits a perturbative solution obtained by means of a path-integral, Hamilton-Jacobi representation.^{11,32,34} In this section, we apply this methodology in order to obtain the corresponding Hamilton-Jacobi-quasi-steady state (HJQSS) approximation.

The (linear) PDE that governs the evolution of the generating function can be written as

$$\frac{\partial G}{\partial t} = H(p_1, \dots, p_n, \partial_{p_1}, \dots, \partial_{p_n})G(p_1, \dots, p_n, t), \quad (19)$$

where the operator H is determined by the reaction rates of the Master Equation (1). Furthermore, the solution to this equation must satisfy the normalisation condition $G(p_1 = 1, \dots, p_n = 1, t) = 1$ for all t .

From the mathematical point of view, Eq. (19) is a Schrödinger-like equation and, therefore, there is a plethora of methods at our disposal in order to analyse it. In particular, when the fluctuations are (assumed to be) small, it is common to resort to WKB methods based on a path integral formulation of the solution of Eq. (19).^{35,36} This approach is based on the WKB-like Ansatz that $G(p_1, \dots, p_n, t) = e^{-S(p_1, \dots, p_n, t)}$. By substituting this Ansatz in Eq. (19) we obtain the following Hamilton-Jacobi equation for the function

$S(p_1, \dots, p_n, t)$:

$$\frac{\partial S}{\partial t} = -H\left(p_1, \dots, p_n, \frac{\partial S}{\partial p_1}, \dots, \frac{\partial S}{\partial p_n}\right). \quad (20)$$

Instead of directly tackling the explicit solution of Eq. (20), we will exploit the Hamilton approach in which, by using the Feynman path-integral representation which yields a solution to Eq. (19) of the type:^{35–37}

$$G(p_1, \dots, p_n, t) = \int_0^t e^{-S(p_1, \dots, p_n, q_1, \dots, q_n, s)} \mathcal{D}q(s) \mathcal{D}p(s), \quad (21)$$

where $\mathcal{D}q(s) \mathcal{D}p(s)$ indicate integration over the space of all possible trajectories and $S(p_1, \dots, p_n, q_1, \dots, q_n)$ given by

$$S(p_1, \dots, p_n, q_1, \dots, q_n) = \int_0^t \left(-H(p_1, \dots, p_n, q_1, \dots, q_n) + \sum_{i=1}^n p_i(s) \dot{q}_i(s) \right) ds, \quad (22)$$

where the position operators in the momentum representation have been defined as $q_i \equiv \partial_{p_i}$ with the commutation relation $[p_i, q_j] = \delta_{i,j}$.

The so-called semi-classical approximation consists of approximating the path integral in Eq. (21) by

$$G(p_1, \dots, p_n, t) = e^{-S(p_1, \dots, p_n, t)}, \quad (23)$$

where p_1, \dots, p_n are now the solution of the Hamilton equations, i.e., the orbits which maximise the action S :

$$\frac{dp_i}{dt} = -\frac{\partial H}{\partial q_i}, \quad (24)$$

$$\frac{dq_i}{dt} = \frac{\partial H}{\partial p_i}, \quad (25)$$

where the pairs (q_i, p_i) are the generalised coordinates corresponding to chemical species $i = 1, \dots, n$. These equations are (formally) solved with boundary conditions³⁰ $q_i(0) = x_i(0)$, where $x_i(0)$ is the initial number of molecules of species i and $p_i(t) = p_i$, where p_i is the momentum corresponding to species i .

A. Michaelis-Menten model of enzyme kinetics

We will now apply this methodology to the enzymatic reaction sketched in Fig. 2 and characterised by the reaction rates given in Table I. Our first step should be to write down the PDE for the characteristic function $G(p_1, p_2, p_3, t)$ defined as

$$G(p_1, p_2, p_3, t) = \sum_{x_1, x_2, x_3} p_1^{x_1} p_2^{x_2} p_3^{x_3} P(x_1, x_2, x_3, t), \quad (26)$$

where x_1, x_2, x_3 are the numbers of molecules of substrate, enzyme, and complex, respectively, and $P(x_1, x_2, x_3, t)$ is the corresponding probability distribution, i.e., the solution of Eq. (1) with rates given in Table I.

The characteristic function PDE is obtained by multiplying both sides of Eq. (1) with rates given in Table I by $p_1^{x_1} p_2^{x_2} p_3^{x_3}$ and summing over all the values of x_1, x_2 , and x_3 .

TABLE II. Dimensionless variables and parameters corresponding to Eqs. (30)–(35). s_0 and e_0 are the initial number of molecules of substrate and enzyme, respectively.

Dimensionless variables	Dimensionless parameters
$\tau = k_1 e_0 t$	$\epsilon = e_0 / s_0$
$z = q_1 / s_0$	$\kappa_2 = k_2 / (k_1 s_0)$
$y = q_2 / e_0$	$\kappa_3 = k_3 / (k_1 s_0)$
$x = q_3 / e_0$	

The result is

$$\begin{aligned} \frac{\partial G}{\partial t} = & k_1(p_3 - p_1 p_2) \frac{\partial^2 G}{\partial p_1 \partial p_2} + k_2(p_1 p_2 - p_3) \frac{\partial G}{\partial p_3} \\ & + k_3(p_2 - p_3) \frac{\partial G}{\partial p_3}, \end{aligned} \quad (27)$$

which implies that the Hamiltonian $H(p_1, p_2, p_3, q_1, q_2, q_3)$ is given by

$$\begin{aligned} H(p_1, p_2, p_3, q_1, q_2, q_3) = & k_1(p_3 - p_1 p_2) q_1 q_2 \\ & + k_2(p_1 p_2 - p_3) q_3 + k_3(p_2 - p_3) q_3. \end{aligned} \quad (28)$$

By rescaling the variables q_i according to transformation shown in Table II, we can rewrite the Hamiltonian Eq. (28) as $H(p, q) = k_1 s_0 e_0 H_k(p, x)$, where

$$\begin{aligned} H_k(p_1, p_2, p_3, z, y, x) = & (p_3 - p_1 p_2) z y + \kappa_2(p_1 p_2 - p_3) x \\ & + \kappa_3(p_2 - p_3) x, \end{aligned} \quad (29)$$

where the variables x, y , and z and the parameters κ_2 and κ_3 are defined in Table II. The corresponding Hamilton equations (24) and (25) in terms of these rescaled variables and defining the dimensionless time, τ , as $\tau = k_1 e_0 t$, read:

$$\frac{dz}{d\tau} = p_2(\kappa_2 x - zy), \quad (30)$$

$$\epsilon \frac{dy}{d\tau} = (\kappa_2 p_1 + \kappa_3) x - p_1 zy, \quad (31)$$

$$\epsilon \frac{dx}{d\tau} = zy - (\kappa_2 + \kappa_3) x, \quad (32)$$

$$\frac{dp_1}{d\tau} = (p_1 p_2 - p_3) y, \quad (33)$$

$$\epsilon \frac{dp_2}{d\tau} = (p_1 p_2 - p_3) z, \quad (34)$$

$$\epsilon \frac{dp_3}{d\tau} = \kappa_2(p_3 - p_1 p_2) + \kappa_3(p_3 - p_2), \quad (35)$$

where $\epsilon = \frac{e_0}{s_0}$ (see Table II).

According to standard arguments in the study of enzyme kinetics,¹ the concentration of substrate, s_0 , is usually orders of magnitude bigger than that of enzyme, e_0 , and therefore $\epsilon = \frac{e_0}{s_0} \ll 1$. This implies that, at the lowest order, the system of equations (30)–(35) becomes:

$$\frac{dz}{d\tau} = p_2(\kappa_2 x - zy), \quad (36)$$

$$(\kappa_2 p_1 + \kappa_3)x - p_1 z y = 0, \quad (37)$$

$$z y - (\kappa_2 + \kappa_3)x = 0, \quad (38)$$

$$\frac{dp_1}{d\tau} = (p_1 p_2 - p_3)y, \quad (39)$$

$$(p_1 p_2 - p_3)z = 0, \quad (40)$$

$$\kappa_2(p_3 - p_1 p_2) + \kappa_3(p_3 - p_2) = 0. \quad (41)$$

This approximation yields a considerable simplification of the system: Eq. (40) implies that $p_1 p_2 - p_3 = 0$, which together with Eq. (39), implies that p_1 is constant. Moreover, Eqs. (40) and (41) lead to $p_2 = p_3$, which, in turn, leads to $p_1 = 1$.

Accordingly, $p_1 = 1$ leads to $x + y = 1$ and therefore $x = z/(z + \kappa_2 + \kappa_3)$, so that Eqs. (36)–(41) reduce to

$$\frac{dz}{d\tau} = -p_3 \frac{\kappa_3 z}{z + \kappa_2 + \kappa_3}, \quad (42)$$

with $p_3 = p_2 = \text{constant}$, $p_1 = 1$, $x = z/(z + \kappa_2 + \kappa_3)$ and $y = 1 - x$. This result allows us to apply the geometrical optics approximation. To do this, we need to calculate the action integral Eq. (22) on its optimal path which is the solution of Eqs. (30)–(35). Note that Eqs. (30)–(35) admit an integral of motion $H(p_1, p_2, p_3, q_1, q_2, q_3) = E = 0$, so that Eq. (22) reads:

$$S(p_1, p_2, p_3, t) = \sum_{i=1}^n \int_0^t q_i(s) \dot{p}_i(s) ds + S(p_1, p_2, p_3, t=0). \quad (43)$$

The corresponding quasi-steady state approximation of the action, which we denote by $S_{QSS}(p_1, p_2, p_3, \tau)$ is given by

$$S_{QSS}(p_1, p_2, p_3, \tau) = s_0 \left(\int_0^\tau z \frac{dp_1}{d\sigma} d\sigma + \int_0^\tau y \left(\epsilon \frac{dp_2}{d\sigma} \right) d\sigma + \int_0^\tau x \left(\epsilon \frac{dp_3}{d\sigma} \right) d\sigma \right) + S(1, p_3, p_3, \tau = 0). \quad (44)$$

Since the quasi-steady state approximation implies that $\epsilon \frac{dp_2}{d\tau} = \epsilon \frac{dp_3}{d\tau} = 0$ which, in turn, leads to $\frac{dp_1}{d\tau} = 0$, $S_{QSS}(p_1, p_2, p_3, \tau)$ reduces to

$$S_{QSS}(p_1, p_2, p_3, \tau) = S(1, p_3, p_3, \tau = 0). \quad (45)$$

Finally, within the geometrical optics approximation, the quasi-steady state characteristic function, $G_{QSS}(p_3, \tau)$ is given by

$$G_{QSS}(p_3, \tau) = e^{-S(1, p_3, p_3, \tau=0)}. \quad (46)$$

Finally, we can obtain the probability distribution function for the total number of enzyme molecules, i.e., those in free form as well as those contained in complexes, u , can be computed using Cauchy's formula:

$$P(e_0, \tau) = \frac{1}{2\pi i} \oint_C \frac{G_{QSS}(p_3, \tau)}{p_3^{e_0+1}} dp_3. \quad (47)$$

The interpretation of this approximation is as follows: The number of molecules of substrate is so much bigger than that of the enzyme that the dynamics of the substrate proceeds

in a quasi-deterministic way (hence $p_1(\tau) = 1$) according to Eq. (42), with stochastic effects being subsumed under the dependence of z on p_3 which modifies the rate of change of z with respect to the mean-field limit (corresponding to $p_3 = 1$). On the other hand, according to Eqs. (45) and (46), the total number of enzyme molecules (i.e., free enzyme plus enzyme in complex molecules), e_0 , whose (average) value is much smaller than the number of substrate molecules, is indeed a random variable, the probability distribution of which stays constant equal to its initial condition.

In order to further clarify the meaning of this approximation, assume that the number of enzyme and complex molecules is initially independent and distributed according to a Poisson distribution with parameter q_2 and q_3 , respectively. Accordingly, the joint characteristic function $G_0(p_2, p_3) = e^{q_2(p_2-1)} e^{q_3(p_3-1)}$ so that $S(1, p_3, p_3, \tau = 0) = -(q_2 + q_3)(p_3 - 1)$. Defining $E \equiv q_2 + q_3$, $S(1, p_3, p_3, \tau = 0) = -E(p_3 - 1)$, the corresponding probability density function is given by

$$P(e_0, \tau) = \frac{1}{2\pi i} \oint_C \frac{e^{E(p_3-1)-e_0 \log p_3}}{p_3} dp_3 = \frac{1}{2\pi i} \oint_C \frac{e^{Ef(p_3)}}{p_3} dp_3, \quad (48)$$

where $f(p_3) = (p_3 - 1) - u_0 \log p_3$ with $u_0 \equiv e_0/E$. Now, if $E \gg 1$, the integral in Eq. (48) can be solved by the method of the steepest descent.^{38,39} According to this method, the dominant contribution to the integral in Eq. (48) comes from the saddle point, i.e., the value of $p_3 = p_0$ such that $f'(p_0) = 0$, i.e., $p_0 = u_0$. In particular, this implies that the rate of change of z , i.e., the scaled number of substrate molecules, is given by Eq. (42) with $p_3 = u_0$. Thus, within this approximation, the rate of change of the number of substrate molecules is regulated by the total number of enzyme molecules.

We can now calculate the average time for the variable z to hit a value, Z , conditioned to initial data $z(t=0) = 1$ and $x(t=0) + y(t=0) = 1$, $T(Z)$. Analytically, we calculate $T(Z)$ by integrating Eq. (42) between $t = 0$ and $T(Z)$, i.e.:

$$T(Z) = (k_1 e_0 \kappa_3 p_3)^{-1} \left(1 - Z + (\kappa_2 + \kappa_3) \log \left(\frac{1}{Z} \right) \right). \quad (49)$$

The accuracy of our analytical result, Eq. (49), is tested in Fig. 4, where it is compared with direct simulations of the corresponding stochastic process (see Table I), for different values of e_0 with $p_3 = u_0 = e_0/E$. We find that there is rather good agreement between theory and simulations, and, as predicted by Eq. (49), the hitting time is inversely proportional to u . Our analytical result, however, appears to slightly overestimate the hitting time $T(Z)$.

B. Optimal fluctuation paths of noise-induced transitions in bistable systems

Once we have established that our asymptotic, Hamilton-Jacobi approximation is able to reproduce with accuracy the actual stochastic dynamics of the Michaelis-Menten model for enzyme kinetics, we can extend our analysis to study the effects of noise in more complex systems which make use of the Michaelis-Menten mechanism and the associated

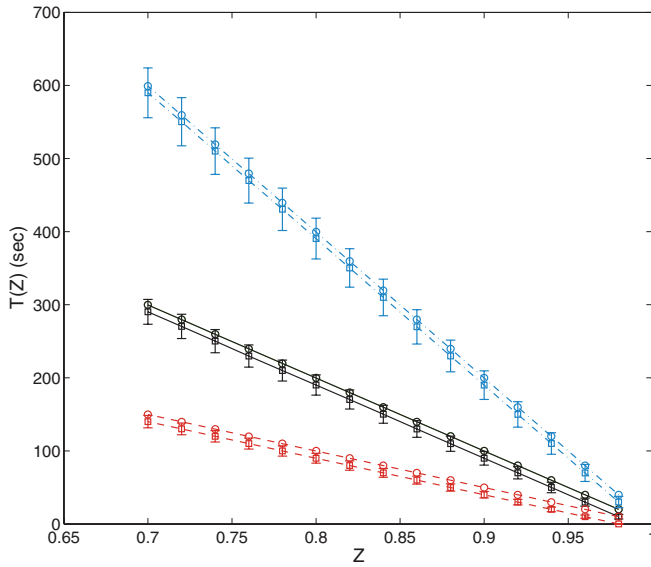
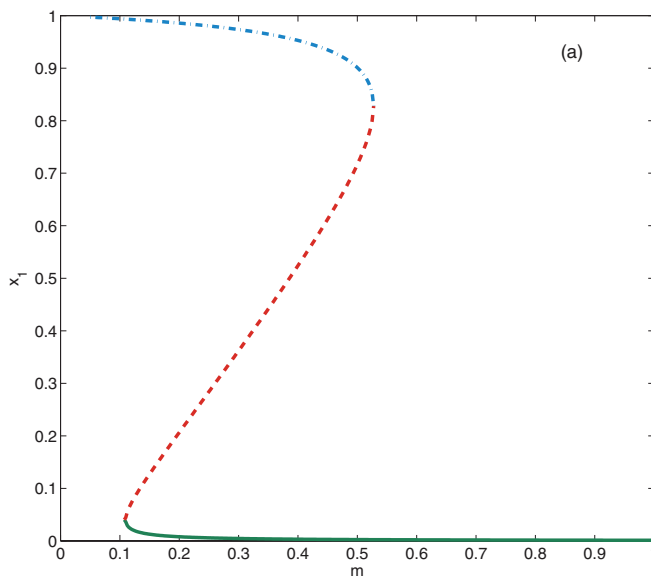


FIG. 4. This figure shows analytical and simulations results for the hitting time $T(Z)$ as a function of the target value, Z , for $E = 10$ and different values of e_0 : Red, dashed lines correspond to $e_0 = 5$, black, solid lines, to $e_0 = 10$, and blue, dotted-dashed lines, to $e_0 = 20$. In all cases, circles correspond to our analytical expression, Eq. (49), whereas squares show results obtained by stochastic simulation using Gillespie's method and averaged over 10 000 realisations for each value of u . Parameter values:¹³ $k_1 = 1$, $k_2 = 1$, $k_3 = 0.1$, $s_0 = \Omega = 1000$.

quasi-steady-state approximation. Examples of such systems are abundant as the Michaelis-Menten approximation is amply used in modelling biochemical pathways.¹ For concreteness, we focus on an example regarding a model of the G_1/S transition in the eukariotic cell-cycle proposed by Tyson and Novak.⁴⁰ In particular, we are interested in ascertaining whether our asymptotic methods can be used to predict the most likely fluctuation path in noise-induced transitions between stable attractors of bistable systems.^{41,42}



For simplicity, we will not consider the full model eukariotic cell-cycle model. Tyson and Novak⁴⁰ have formulated a model such that the core of the system regulating progression of the cell-cycle through the G_1/S transition is a system of two, mutually repressing proteins. This system of mutual repression gives rise to a bistable system where one of the stable steady states is identified with the G_1 phase whereas the other corresponds to a state where the cell is ready to go through the other three phases of the cell-cycle, known as S, G_2 , and M. This central module, which is the one we are focus on, is acted upon by a complex regulatory network which monitors if conditions are met for the cell to undergo this transition and accounts for its accurate timing. Presently, we ignore this network and focus on the central bistable system, whose (mean-field) dynamics is determined by

$$\begin{aligned} \frac{dx_1}{dt} &= \frac{a_3(1-x_1)}{J_3 + (1-x_1)} - \frac{a_4 m x_7 x_1}{J_4 + x_1}, \\ \frac{dx_7}{dt} &= a_1 - (a'_2 + a''_2 x_1) x_7, \end{aligned} \quad (50)$$

where x_7 represents the concentration cyclin-B/CDK dimers, an activator of cell-cycle progression, x_1 is the concentration of active Cdh1/APC complexes, which hinders the G_1/S transition, and m is the size (mass) of the cell. Parameter values are chosen so that both variables $0 \leq x_1, x_7 \leq 1$.

A summary of the properties of the phase space of the system of ODEs (Eq. (50)) is given in Fig. 5, where we show its bifurcation diagram taking the cell-size, m , as the control parameter (Fig. 5(a)) as the null-clines corresponding to $m = 0.4$ (Fig. 5(b)). We observe that, for the parameter values considered, there are three points where the null-clines intersect, corresponding two stable attractors and an unstable saddle point. The two stable attractors correspond to the so-called G_1 -point ($x_1 \sim 1, x_7 \sim 0$, blue dashed-dotted line in Fig. 5(a)) and the S- G_2 -M point ($x_1 \sim 0, x_7 \sim 1$, green solid line in

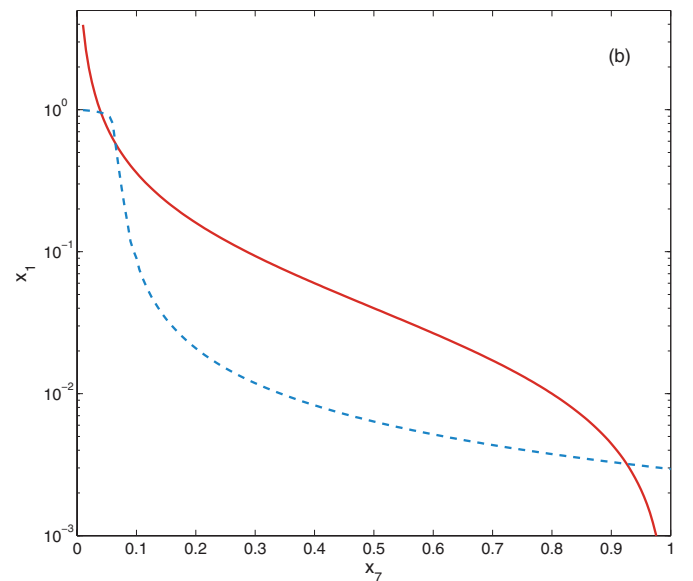


FIG. 5. (a) Bifurcation diagram for the Tyson and Novak system, Eq. (50). Blue dashed-dotted and green solid lines correspond to the (stable) G_1 branch and the (stable) S- G_2 -M, respectively, while the red dashed line represents the unstable branch. (b) Null-clines for the Tyson and Novak system, Eq. (50). The red solid line corresponds to the x_7 -null-cline whereas the blue dashed line is the x_1 -null-cline. We have taken $m = 0.4$. Other parameter values are given in Table V, Appendix B.

TABLE III. Transition rates corresponding to the enzymatic reaction shown in Fig. 6.

Transition rate	r	Event
$W_1(x) = k_1 x_7 x_1 x_3$	$r_1 = (-1, 0, -1, 0, +1, 0, 0)$	Enzyme and active Cdh1 form complex
$W_2(x) = k_2 x_7 x_5$	$r_2 = (+1, 0, +1, 0, -1, 0, 0)$	Enzyme-active Cdh1 complex splits
$W_3(x) = k_3 x_7 x_5$	$r_3 = (0, +1, +1, 0, -1, 0, 0)$	Inactivation of Cdh1 and enzyme release
$W_4(x) = k_4 x_2 x_4$	$r_4 = (0, -1, 0, -1, 0, +1, 0)$	Enzyme and inactive Cdh1 form complex
$W_5(x) = k_5 x_6$	$r_5 = (0, +1, 0, +1, 0, -1, 0)$	Enzyme-inactive Cdh1 complex splits
$W_6(x) = k_6 x_6$	$r_6 = (+1, 0, 0, +1, 0, -1, 0)$	Inactivation of Cdh1 and enzyme release
$W_7(x) = k_7$	$r_7 = (0, 0, 0, 0, 0, 0, +1)$	CycB synthesis
$W_8(x) = k_8(1 + \alpha x_1) x_7$	$r_8 = (0, 0, 0, 0, 0, 0, -1)$	CycB degradation

Fig. 5(a)). In between these two, with intermediate values of both variables, there is an unstable saddle point (red dashed line in Fig. 5(a)). The basins of attraction of both attractors are disjoint sets of the phase plane, separated by a separatrix that passes through the saddle point.⁴⁰ When noise is ignored, the initial condition fully determines to which attractor the trajectory is going to converge. In contrast, when noise is considered, it introduces the possibility of random convergence to either of the (deterministically) stable attractors and stochastic switching between them.

1. Stochastic model and HJQS approximation

We have shown in Ref. 43 that the mean-field limit of the stochastic, law-of-mass action model given in Table III (schematically shown in Fig. 6) leads to Eq. (50). We now apply the same methodology as in Sec. III A to the model given in Table III. Using this methodology the corresponding Hamiltonian, H , is given by

$$H(x_1, \dots, x_7, p_1, \dots, p_7) = H_A + H_I + H_B, \quad (51)$$

where the H_A is the Hamiltonian corresponding to the enzymatic activation of Cdh1 (reactions 1 to 3 in Table III):

$$\begin{aligned} H_A(x_2, x_4, x_6, p_1, p_2, p_4, p_6) \\ = k_4(p_6 - p_2 p_4) x_2 x_4 + k_5(p_2 p_4 - p_6) x_6 + k_6(p_1 p_4 - p_6) x_6, \end{aligned} \quad (52)$$

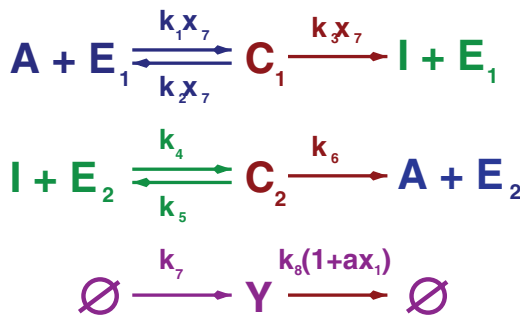


FIG. 6. Enzymatic reactions leading to Eq. (50) in the quasi-steady state approximation. A represents active Cdh/Apc (x_1), I, inactive Cdh/Apc (x_2), E_1 , activating enzymes (x_3), E_2 , inactivating enzymes (x_4), C_1 , active Cdh/Apc- E_1 complexes (x_5), C_2 , inactive Cdh/Apc- E_2 complexes (x_6), and Y the number of CycB-CDK complexes (x_7). The first two reactions correspond to enzyme-catalysed activation and inactivation of Cdh/APC. The third reaction corresponds to the dynamics of CycB activity: synthesis at a constant rate, k_7 , and degradation by natural decay and active Cdh/APC-induced inactivation.

H_I corresponds to CycB-regulated enzymatic inactivation of Cdh1 (reactions 4 to 6 in Table III):

$$\begin{aligned} H_I(x_1, x_3, x_5, x_7, p_1, p_2, p_3, p_5, p_7) \\ = k_1 p_7 (p_5 - p_1 p_3) x_1 x_3 x_7 + k_2 p_7 (p_1 p_3 - p_5) x_5 x_7 \\ + k_3 p_7 (p_2 p_3 - p_5) x_5 x_7, \end{aligned} \quad (53)$$

and, last, H_B , which corresponds to synthesis and degradation of CycB, is given by (reactions 7 to 8 in Table III):

$$\begin{aligned} H_B(x_1, x_7, p_1, p_7) = k_7(p_7 - 1) + k_8(1 - p_7) x_7 \\ + k_8 \alpha p_1 (1 - p_7) x_1 x_7, \end{aligned} \quad (54)$$

In the rescaled/dimensionless variables of Table IV, the Hamiltonian equation (51) is given by $H = k_1 s_0 e_0 y_0 (H_{A_k} + H_{I_k} + H_{B_k})$, where H_{A_k} , H_{I_k} , and H_{B_k} are given by

$$\begin{aligned} H_{A_k} &= \kappa_4(p_6 - p_2 p_4) \hat{x}_2 \hat{x}_4 + \kappa_5(p_2 p_4 - p_6) \hat{x}_6 + \kappa_6(p_1 p_4 - p_6) \hat{x}_6, \\ H_{I_k} &= p_7(p_6 - p_2 p_4) \hat{x}_1 \hat{x}_3 \hat{x}_7 + \kappa_2 p_7 (p_1 p_3 - p_5) \hat{x}_5 \hat{x}_7 \\ &\quad + \kappa_3 p_7 (p_2 p_3 - p_5) \hat{x}_5 \hat{x}_7, \\ H_{B_k} &= \kappa_7(p_7 - 1) + \kappa_8(1 - p_7) \hat{x}_7 + \kappa_8 \alpha p_1 (1 - p_7) \hat{x}_1 \hat{x}_7, \end{aligned} \quad (55)$$

As in the standard Michaelis-Menten kinetics analysed in Sec. III A, we assume that the $s_0 \gg e_0$ and therefore $\epsilon \ll 1$. This leads to the following quasi-steady state approximation (see Appendix B for a detailed derivation):

$$\frac{dx_1}{d\tau} = p_4 \frac{\kappa_4 x_2}{x_2 + J_2} - p_7 p_3 \frac{\kappa_3 x_7 x_1}{x_1 + J_1} + \kappa_8 \alpha (1 - p_7) x_7 x_1, \quad (56)$$

$$\frac{dx_2}{d\tau} = -p_4 \frac{\kappa_4 x_2}{x_2 + J_2} + p_7 p_3 \frac{\kappa_3 x_7 x_1}{x_1 + J_1}, \quad (57)$$

$$\frac{dx_7}{d\tau} = \kappa_7 - \kappa_8(1 + \alpha p_1 x_1) x_7, \quad (58)$$

$$p_1 = p_2 = \frac{\kappa_7 - \kappa_8 x_7}{\kappa_8 \alpha x_1 x_7}, \quad (59)$$

$$p_5 = p_3 p_1, \quad (60)$$

$$p_6 = p_4 p_1, \quad (61)$$

$$\frac{dp_7}{d\tau} = -(1 - p_7) \kappa_8 (1 + \alpha p_1 x_1), \quad (62)$$

TABLE IV. Dimensionless variables used in Eqs. (B1)–(B7) and Eqs. (B8)–(B14). s_0 , e_0 , and y_0 are the total concentration of Cdh1, the total concentration of activating and inactivating enzymes, and the stationary concentration of active CycB, respectively. For simplicity in the notation, the hats in the dependent variables in Eqs. (B1)–(B7) have been dropped.

Dimensionless variable	Dimensionless parameters
$\tau = k_1 e_0 y_0 t$	$\epsilon = e_0/s_0$
$\hat{x}_1 = x_1/s_0$	$\kappa_2 = k_2/(k_1 s_0)$
$\hat{x}_2 = x_2/s_0$	$\kappa_3 = k_3/(k_1 y_0)$
$\hat{x}_3 = x_3/e_0$	$\kappa_4 = k_4/(k_1 s_0 y_0)$
$\hat{x}_4 = x_4/e_0$	$\kappa_5 = k_5/(k_1 s_0 y_0)$
$\hat{x}_5 = x_5/e_0$	$\kappa_6 = k_6/(k_1 e_0 y_0)$
$\hat{x}_6 = x_6/e_0$	$\kappa_7 = k_8/(k_1 e_0 y_0 s_0)$
$\hat{x}_7 = x_7/y_0$	$\kappa_8 = k_8/(k_1 e_0 y_0)$, $\alpha = a s_0$

where, to simplify the notation, we have dropped the hats for the rescaled variables. Equation (59) has been obtained from the fact that the stochastic trajectories are constrained to constant energy (i.e., constant H) manifolds, in particular, stochastic trajectories must be such that $H = 0$. Since $H_A = H_B = 0$ (see Appendix B), $H = k_1 s_0 e_0 y_0 H_{QSS} = 0$ with $H_{QSS} = (1 - p_7)(-\kappa_7 + \kappa_8(1 + \alpha p_1 x_1) x_7)$. Equation (59) follows from $H_{QSS} = 0$.

2. QSS approximation of the action functional

As discussed in previously, the action functional is given by

$$S(p, t) = - \sum_i \int_0^t x_i \frac{dp_i}{d\sigma} d\sigma + S_0(p), \quad (63)$$

where $S_0(p) = S(p, t = 0)$. In terms of the rescaled variables shown in Table IV, and taken into account that we have taken $s_0 = y_0$, the action functional reads:

$$S(p, \tau) = -s_0 \left(\int_0^\tau x_1 \frac{dp_1}{d\sigma} d\sigma + \int_0^\tau x_2 \frac{dp_2}{d\sigma} d\sigma + \sum_{i=3}^6 \int_0^\tau x_i \left(\epsilon \frac{dp_i}{d\sigma} \right) d\sigma + \int_0^\tau x_7 \frac{dp_7}{d\sigma} d\sigma \right) + S_0(p). \quad (64)$$

As per the QSS approximation (see Appendix B), $\epsilon \dot{p}_i \approx 0$ $i = 2, \dots, 6$, so that $S(p, \tau)$ can be approximated by $S_{QSS}(p, \tau)$ given by

$$S_{QSS}(p, \tau) = -s_0 \left(\int_0^\tau x_1 \frac{dp_1}{d\sigma} d\sigma + \int_0^\tau x_2 \frac{dp_2}{d\sigma} d\sigma + \int_0^\tau x_7 \frac{dp_7}{d\sigma} d\sigma \right) + S_0(p). \quad (65)$$

Furthermore, from Eqs. (56) and (57), we note that in order for the total concentration of Cdh1 (active plus inactive form) to be conserved $p_7(\tau) = 1$, so that $\dot{p}_7 = 0$. We also note that, from Appendix B, Eqs. (B33)–(B36), $p_1 = p_2$. By partial integration of the first two integrals on the right-hand side of Eq. (65), and using that $x_1 + x_2 = 1$ and, therefore,

$\dot{x}_1 + \dot{x}_2 = 0$, so that:

$$S_{QSS}(p, \tau) = -s_0 (p_1(\tau) - p_1(0)) + S_0(p). \quad (66)$$

Similar to the stochastic QSS approximation of the Michaelis-Menten system, Eq. (42), we note that the QSS approximation leaves two degrees of freedom in Eqs. (56)–(62), i.e., the values of p_3 and p_4 , i.e., the momenta corresponding to the number of Cdh1-inactivating enzymes and Cdh1-activating enzymes, respectively, which fix the time scales of activation and inactivation of the Cdh1 molecules. Otherwise, the remaining momenta are fixed by the QSS approximation: $p_1 = p_2$ are determined by x_1 and x_7 and p_5 and p_6 are determined by p_1 , p_3 , and p_4 (see Appendix B). Therefore, as far as the determination of p_3 and p_4 is concerned, no information is lost by taking $p_1 = p_2 = 1$ in Eq. (65), so that $S_{QSS}(p_3, p_4) \equiv S_{QSS}(p_1 = 1, p_2 = 1, p_3, p_4, p_5 = 1, p_6 = 1)$:

$$S_{QSS}(p_3, p_4, \tau) = S_3(p_3) + S_4(p_4), \quad (67)$$

where we have assumed that the initial number of active Cdh1-inactivating enzyme and inactive Cdh1-active enzyme complexes are independent random variables. $S_3(p_3)$ and $S_4(p_4)$ correspond to the generating functions for probability distribution of the initial values $x_3(\tau = 0)$ and $x_4(\tau = 0)$. In order to determine p_3 and p_4 we use the same method as the one we used for the Michaelis-Menten model, namely, p_3 and p_4 are given by a stationary phase argument (see Sec. III A). Following the same methodology, we find that p_3 and p_4 are the roots of equations:

$$p_3 \frac{dS_3}{dp_3} = x_3(\tau = 0), \quad (68)$$

$$p_4 \frac{dS_4}{dp_4} = x_4(\tau = 0).$$

Assuming that $x_3(\tau = 0)$ and $x_4(\tau = 0)$ are Poisson random variables with $E = \langle x_i(\tau = 0) \rangle$, $i = 3, 4$, then $p_3 = x_3(\tau = 0)/E$ and $p_4 = x_4(\tau = 0)/E$. This result, as well as the equivalent one for the Michaelis-Menten system, confirms that unlike its mean-field counterparts, the QSS approximation of the stochastic system retains a dependence on the initial values of the number enzyme molecules. An example of the implications of this prediction is shown in Fig. 7(a), in which we show that, within our HJQSS approximation, initial conditions within the G_1 -basin of attraction exhibit faster decay towards the S- G_2 -M-attractor as $p_3 = p_4$ increases. Therefore, according to our analysis, the average exit time, $T_E(Z)$, defined as the average time the stochastic dynamics take to reach the boundary of a domain given by $x_1 \leq Z$, should be a decreasing function of the initial number of enzyme molecules. This prediction is confirmed by direct simulation of the stochastic dynamics by means of Gillespie's SSA (see Fig. 7(b)).

3. Fluctuation paths and optimal escape trajectories

We now address the problem of computing fluctuation paths with a focus on the optimal trajectories of noise-induced escape from the stable steady states of the mean-field dynamics, Eq. (50) and shown in Fig. 5. In particular, we will study

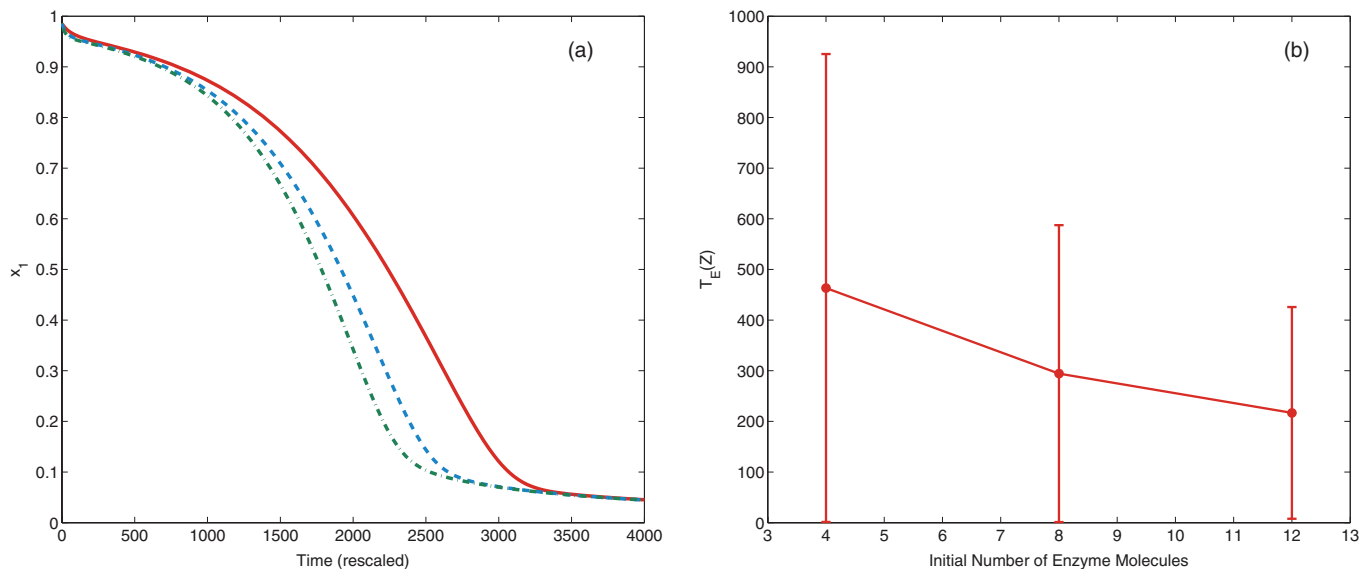


FIG. 7. (a) Numerical solution of the HJQSS approximation, Eqs. (56)–(62), for different values of p_3 and p_4 . We observe in this graph that as p_3 and p_4 are let to grow, the exit time from the G_1 attractor decreases. Key: solid red line corresponds to $p_3 = p_4 = 3$, blue dashed line, to $p_3 = p_4 = 6$, and green dashed-dotted line, to $p_3 = p_4 = 9$. (b) Simulation results showing the dependence of the average exit time $T_E(Z)$ with $Z = 0.1$. The error bars in plot (b) correspond to ± 1 standard deviation with respect to the mean, as calculated from the data obtained by direct simulation of the process using Gillespie's stochastic simulation algorithm. We have checked from our simulation results that the waiting time for the transition from the G_1 to S-G2-M, T_w , is exponentially distributed with mean equal to T_E , i.e., $P(T_w) = T_E^{-1} e^{-T_w/T_E}$. For such distribution, the standard deviation, σ_w , given by the square root of the variance, and the mean are equal: $\sigma_w = T_E$. Initial conditions: $x_1 = 0.9858$ and $x_7 = 0.0390$, $m = 0.4$. Parameter values are given in Table V, Appendix B.

the escape from the G_1 -steady state ($x_1 \sim 1$, $x_2 \sim 0$, and $x_7 \sim 0$) into the S-G2-M steady state ($x_1 \sim 0$, $x_2 \sim 0$, and $x_7 \sim 1$).

Figure 8(a) shows that the numerical solution of Eqs. (56)–(62) with $p_5 = p_6 = p_7 = 1$ and the G_1 -state as initial condition for x_1 , x_2 , and x_7 . The solution corresponds to a trajectory connecting the G_1 state and the S-G2-M state, which by construction is the quasi-steady state approximation to the optimal (in the sense of more likely) noise-induced escape path. In order to ascertain the accuracy of our approximation, we have compared these asymptotic result to direct Monte Carlo (Gillespie) simulations of the (full) stochastic process shown in Table III. Figure 8(a) shows individual realisations of the stochastic dynamics in which the system escapes from the G_1 state. We find good agreement

between Gillespie simulations and the solution of system, Eqs. (56)–(62).

Furthermore, we have computed other fluctuation paths with different initial conditions (see Figs. 8(b) and 8(c)) by numerically solving Eqs. (56)–(62). Comparing with individual realisations obtained by direct stochastic simulations, we find that there is good agreement in these two other cases too.

Note that the HJQSS equations (56)–(62) predict the most likely fluctuation path. It is therefore perfectly consistent with our method, that, albeit less likely, paths that differ from the HJQSS trajectory are also found. In particular, our HJQSS approximation of the Tyson and Novak system, Eq. (50), is unable to predict fluctuations which involve transient sojourns into the basin of attraction of the G_1 fixed point. As shown in Fig. 9, such trajectories exist and are found with

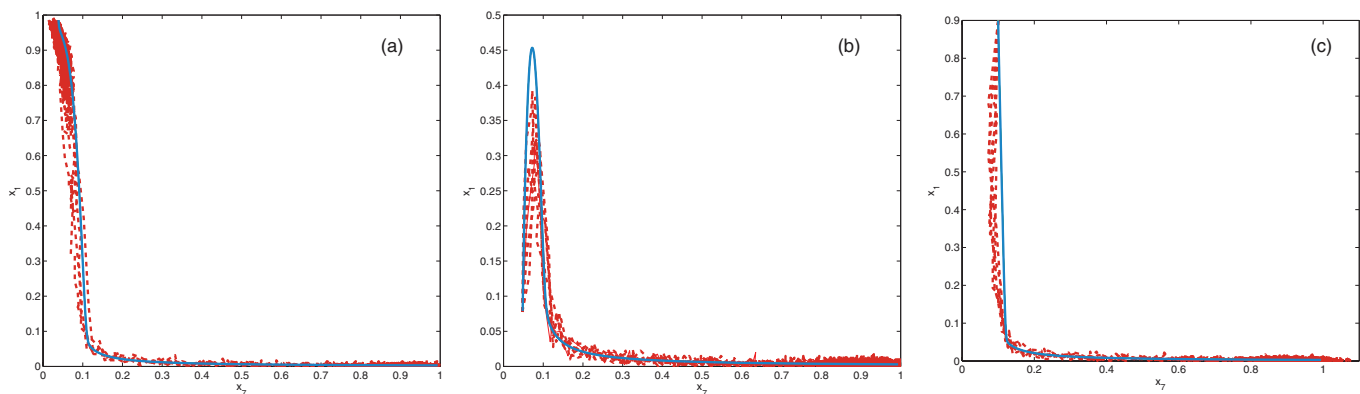


FIG. 8. Comparison between the theoretical most probable fluctuation path and simulation results, $\Omega = 400$. Initial condition: (a) $x_1 = 0.9858$ and $x_7 = 0.0390$, (b) $x_1 = 0.0790$ and $x_7 = 0.0482$, and (c) $x_1 = 0.9$ and $x_7 = 0.1$. $p_3 = p_4 = 3$. Each theoretical curve is compared to 5 stochastic sample paths obtained by direct simulation, $m = 0.4$. Parameter values are given in Table V, Appendix B.

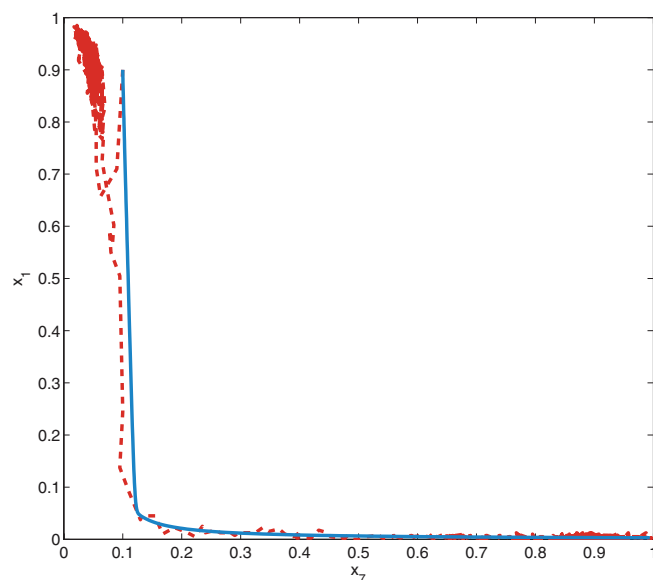


FIG. 9. Fluctuation path for the stochastic Tyson and Novak system with initial condition $x_1 = 0.9$ and $x_7 = 0.1$ (red dashed line). This initial condition is very close to the deterministic separatrix of the mean-field system (Eq. (50)), but belonging to the basin of attraction of the S-G₂-M fixed point. Although the HJQSS approximation predicts that the most likely fluctuation path (blue solid line) is relaxation onto the S-G₂-M fixed-point, this figure shows a realisation where the system makes a sojourn into the G₁ attractor before relaxing onto S-G₂-M fixed-point. Parameter values are given in Table V, Appendix B.

small frequency in stochastic simulations. Although, as predicted by our HJQSS, these trajectories eventually relax onto the S-G₂-M-like, HJQSS attractor (see Fig. 9), our HJQSS approximation does not reproduce the transient G₁-excursions.

IV. CONCLUSIONS

In this paper, we have introduced two asymptotic methods to study the quasi-steady state approximation in stochastic systems described by the master equation. Both methods are based in a WKB/large deviations Ansatz for the characteristic function and for the generating function associated to the probability distribution of the system. We have developed a multi-scale WKB approximation, which is a generalisation of the WKB method introduced by Kubo *et al.*¹¹ To the lowest order, this method provides a Gaussian approximation, in terms of the lowest order terms of the asymptotic expansions for the first and second cumulants (mean value and variance, respectively). These quantities are determined by a system of ODEs such that, when the variables are properly rescaled, leads to a system where the quasi-steady approximation can be readily applied (see Eq. (A23)). In turn, applying the QSS approximation to Eq. (A23) leads to a system of equations (Eqs. (8) and (9)) which is a generalisation of the deterministic QSS approximation.

The second method is based on a HJQSS approximation, where we exploit the Hamilton-Jacobi representation of the process described by the master equation (Eq. (1)). This representation, based on the path-integral solution of the partial differential equation for the generating function,^{11,30,32,35,36} allows us to compute the optimal transition path between

two states solving the corresponding Hamilton equations. By rescaling both the random variables and time, we obtain a system to which the QSS approximation can be applied (see Eqs. (B1)–(B14)) resulting in the HJQSS approximation, Eqs. (56)–(62), and the corresponding QSS approximation to the optimal transition path between two states. This approximation allows to predict that, unlike the corresponding QSS approximation in the mean-field limit, the behaviour of the stochastic system depends on the initial concentration of enzymes/complexes (see, for example, Fig. 4). This prediction is fully corroborated by comparison with Gillespie stochastic simulations.

These two methods provide complementary information about the process. Whereas the MSWKB approximation provides an approximation to the full probability distribution, the HJQSS produces only the optimal transition trajectories between two states. However, whereas our current lowest-order MSWKB allows to study only small deviations with respect to the mean value (see Fig. 3), the HJQSS enables us to study rare events and large deviations with respect to the mean, such as transitions between two attractors of a bistable system (see Fig. 8(a)).

Both our methods have been shown to exhibit limitations. The lowest-order MSWKB approximation, where only the lowest order approximation to the first and second cumulants is considered to formulate a Gaussian approximation, has been shown to break down in the long time limit, where our Gaussian approximation fails to describe the statistics of the process with accuracy (see Fig. 3(b)). Regarding the HJQSS approximation, it provides the most likely fluctuation path between two states of the system. Whereas this information is valuable and allows to compute quantities such as the transition time between the two states,³⁰ which carry important information about the behaviour of the system, it is only a partial description of the system. For example, for the particular choice of initial conditions shown in Fig. 9, we have seen that our HJQSS approximation to study the stochastic behaviour of the Tyson and Novak system (50) precludes the possibility of transitions from the S-G₂-M basin of attraction to the G₁ basin of attraction, we have shown by means of direct stochastic simulation that such transitions are possible albeit transient and infrequent: Transient sojourns from the S-G₂-M to the G₁ basin of attractions occur although they eventually relax until they reach the S-G₂-M-like HJQSS attractor (see Fig. 9).

Improving these approximations is possible. In the case of the MSWKB approximation, this method can be improved in a straightforward manner by (i) computing higher order cumulants to go beyond the Gaussian approximation, and (ii) to compute the higher-order corrections to the cumulants.¹¹ An alternative formulation of the MSWKB method presented here would consist of considering the use of Van Kampen's system-size expansion,¹⁰ also known as the linear noise approximation (LNA), which is closely related to Kubo *et al.*¹¹ WKB approximation. In spite of the similarities between both methodologies, they are not exactly equivalent. The LNA assumes that the random variable can be written as $X(t) = \phi(t) + \Omega^{1/2}\xi(t)$, where $\phi(t)$ is the solution of the mean-field equations and $\xi(t)$ is a random variable

which satisfies a linear Fokker-Planck equations from where (linear) ordinary differential equations for the first and second moments of $\xi(t)$ can be derived. The WKB approximation is based on an Ansatz regarding the form of the solution of the Master Equation, which means that, as far as our results are concerned, the equations for the variance of $X(t)$ are not, in general, the same, although the same mean-field approximation is obtained in both cases. Moreover, a multi-scale LNA would involve finding a way of dealing with the fact that different species scale differently with system similarly to the method developed by Thomas *et al.* using projector operator techniques.⁸ Regarding the HJQS approximation, its predictions could be improved by using methods to sample the ensemble of transition paths,^{44–46} which provide much information beyond the one provided by the most probable transition paths. These extensions of the methodologies presented in this paper will be the subject of future research.

ACKNOWLEDGMENTS

T.A. thanks Pilar Guerrero and Roberto de la Cruz for useful comments. T.A. gratefully acknowledges the Spanish Ministry for Science and Innovation (MICINN) for funding under Grant No. MTM2011-29342 and Generalitat de Catalunya for funding under Grant No. 2009SGR345.

APPENDIX A: DERIVATION OF THE LOWEST ORDER MSWKB APPROXIMATION

This appendix is devoted to the derivation of Eqs. (8) and (9). Recall that the rescaled master equation for the characteristic function reads:

$$\frac{1}{\Omega^{\alpha_0}} \frac{\partial Q(u, t)}{\partial t} = \frac{1}{(2\pi)^d} \sum_i (e^{-iu \cdot y_i} - 1) \times \int_{-\infty}^{\infty} \Omega^{\beta_i - \alpha_0} w_i(v) Q(u - v, t) dv, \quad (\text{A1})$$

where $w_i(u) = \int_{-\infty}^{\infty} a_i(z) e^{iu \cdot z} dz$. Using the definition of the cumulant-generating function in terms of the characteristic function: $Q(u, t) = \exp(q(u, t))$ and Eq. (6) we obtain:

$$\frac{1}{\Omega^{\alpha_0}} \sum_{n=1}^{\infty} \frac{i^n}{n!} u^n \cdot \frac{dq_n}{dt} = \frac{1}{(2\pi)^d} \sum_{n=1}^{\infty} \frac{(-iu \cdot y_i)^n}{n!} \times \sum_i \int_{-\infty}^{\infty} \Omega^{\beta_i - \alpha_0} w_i(v) \frac{Q(u - v, t)}{Q(u, t)} dv. \quad (\text{A2})$$

In order to proceed further, note that $Q(u - v, t) = e^{q(u - v, t)} = e^{e^{(u - v) \cdot \partial_v} q(-v, t)}$ so that $Q(u - v, t) = \exp(\sum_n \frac{1}{n!} (u \cdot \partial_v)^n q(-v, t))$. Taking this into account, it is straightforward to express the ratio $\frac{Q(u - v, t)}{Q(u, t)}$ as

$$\frac{Q(u - v, t)}{Q(u, t)} = \exp\left(\sum_{n=0}^{\infty} \frac{i^n}{n!} h_n(-v, t)\right), \quad (\text{A3})$$

where $h_n(-v, t) = i^{-n}((u \cdot \partial_v)^n q(-v, t) - (u \cdot \partial_v)^n q(-v, t)|_{v=0})$. This expression together with $h_n(-v, t) = q(-v, t)$

allows us to rewrite Eq. (A2) as

$$\begin{aligned} & \frac{1}{\Omega^{\alpha_0}} \sum_{n=1}^{\infty} \frac{i^n}{n!} u^n \cdot \frac{dq_n}{dt} \\ &= \frac{1}{(2\pi)^d} \sum_{n=1}^{\infty} \frac{(-iu \cdot y_i)^n}{n!} \\ & \times \sum_i \int_{-\infty}^{\infty} \Omega^{\beta_i - \alpha_0} e^{(\sum_{n=1}^{\infty} \frac{i^n}{n!} h_n(-v, t))} e^{q(-v, t)} w_i(v) dv. \quad (\text{A4}) \end{aligned}$$

We further define the quantities $m_n(v, t)$ by means of the relation:

$$\exp\left(\sum_{j=1}^{\infty} \frac{i^j}{j!} h_j(-v, t)\right) = \sum_{n=0}^{\infty} \frac{i^n}{n!} u^n \cdot m_n(v, t). \quad (\text{A5})$$

According to this definition $m_0(v, t) = 1$. Equation (A2) can be rewritten as

$$\begin{aligned} & \frac{1}{\Omega^{\alpha_0}} \sum_{n=1}^{\infty} \frac{i^n}{n!} u^n \cdot \frac{dq_n}{dt} \\ &= \frac{1}{(2\pi)^d} \sum_{n=1}^{\infty} \frac{(-iu \cdot y_i)^n}{n!} \\ & \times \sum_i \int_{-\infty}^{\infty} \Omega^{\beta_i - \alpha_0} \sum_{n=0}^{\infty} \frac{i^n}{n!} u^n \cdot m_n(v, t) w_i(v) e^{q(-v, t)} dv. \quad (\text{A6}) \end{aligned}$$

Equation (A6) provides evolution equations for each of the cumulants of $P(z, t)$, which are obtained by going through the different $O(u^n)$ -orders. For example, the equations for the first cumulant $q_1(t) = \langle z(t) \rangle$ are given by the $O(u)$ terms in Eq. (A6):

$$\frac{ds_j}{dt} = \frac{\Omega^{\alpha_0 - \alpha_j}}{(2\pi)^d} \sum_i \int_{-\infty}^{\infty} \Omega^{\beta_i - \alpha_0} e^{q(-v, t)} r_{i,j} w_i(v) dv, \quad (\text{A7})$$

where s_j and the components of $q_1 = (q_{1,j})$ are related by: $q_{1,j} = s_j + o(\Omega^{-\alpha_j})$ and $y_i = (y_{ij})$ with $y_{ij} = \Omega^{-\Omega_j} r_{ij}$. Let j_0 be such that $\alpha_{j_0} = \alpha$. Furthermore, let $\alpha_1 = \max_j \alpha_j$ and j_1 be such that $\alpha_{j_1} = \alpha_1$, so that:

$$\frac{ds_j}{dt} = \frac{\Omega^{\alpha_0 + \alpha_1 - \alpha_j}}{(2\pi)^d} \sum_i \int_{-\infty}^{\infty} \Omega^{\beta_i - \alpha_0 - \alpha_1} e^{q(-v, t)} r_{i,j} w_i(v) dv. \quad (\text{A8})$$

We further define the rescaled time variable τ as $t = \Omega^{-\alpha_0} \tau$ and rescale the rate constants so that $v_i(v) = \Omega^{\beta_i - \alpha_0 - \alpha_1} w_i(v)$, we obtain:

$$\begin{aligned} & \frac{1}{\Omega^{\alpha_1 - \alpha_j}} \frac{ds_j}{d\tau} = \frac{1}{(2\pi)^d} \sum_i \int_{-\infty}^{\infty} e^{q(-v, \tau)} r_{i,j} v_i(v) dv \text{ if } j \neq j_1, \\ & \frac{ds_{j_1}}{d\tau} = \frac{1}{(2\pi)^d} \sum_i \int_{-\infty}^{\infty} e^{q(-v, \tau)} r_{i,j_1} v_i(v) dv \text{ if } j = j_1. \quad (\text{A9}) \end{aligned}$$

Similarly, we can obtain the equations for the components of the second cumulant, i.e., the covariance matrix, $q_{2,jk}(t) = \langle z_j z_k \rangle - \langle z_j \rangle \langle z_k \rangle$. Assuming that the entries of

the covariance matrix scale as $q_{2,jk}(t) = \Omega^{-\frac{\alpha_j - \alpha_k}{2}} S_{jk}(t) + o(\Omega^{-\frac{\alpha_j - \alpha_k}{2}})$, as $q_{2,jk}$ must be symmetric and that $m_{1,k}(v, t) = \Omega^{-\alpha_k} M_{1,k}(v, t) + o(\Omega^{-\alpha_0})$:^{11,29}

$$\frac{dq_{2,jk}}{dt} = \frac{\Omega^{\alpha_1 + \alpha_0 - \alpha_j - \alpha_k}}{(2\pi)^d} \sum_i \int_{-\infty}^{\infty} (r_{i,j} M_{1,k}(v, t) + r_{i,k} M_{1,j}(v, t) + r_{i,j} r_{i,k}) e^{q(-v,t)} v_i(v) dv. \quad (\text{A10})$$

Furthermore, by rescaling time as $t = \Omega^{-\alpha_0} \tau$, Eq. (A10) reads:

$$\frac{dq_{2,jk}}{d\tau} = \frac{\Omega^{\alpha_1 - \alpha_j - \alpha_k}}{(2\pi)^d} \sum_i \int_{-\infty}^{\infty} (r_{i,j} M_{1,k}(v, \tau) + r_{i,k} M_{1,j}(v, \tau) + r_{i,j} r_{i,k}) e^{q(-v,\tau)} v_i(v) dv. \quad (\text{A11})$$

In order to complete our derivation of Eqs. (A9) and (A11) we need to obtain $q(-v, \tau)$ and $m_1(v, \tau)$ to the lowest order of approximation. Recall that $q(-v, t) = -i v \cdot q_1 + \frac{(iv)^2}{2} \cdot q_2 + o(\Omega^{-\alpha_0})$ and that, from the definition of the quantity $h_n(-v, \tau)$:²⁹

$$m_1(v, \tau) = \partial_v q(-v, \tau) - \partial_v q(-v, \tau)|_{v=0}. \quad (\text{A12})$$

Therefore, to the lowest order:

$$m_1(v, \tau) = \frac{1}{2} \partial_v (v^2 \cdot q_2), \quad (\text{A13})$$

which, in components, reads $m_{1,k}(v, \tau) = \sum_l (v_l q_{2,lk} + v_l q_{2,kl}) = 2 \sum_l v_l q_{2,kl}$, where we have used that q_2 must be a symmetric matrix. In order for $m_1(v, \tau)$ to satisfy the scaling Ansatz $m_{1,k}(v, t) = \Omega^{-\alpha_k} M_{1,k}(v, t) + o(\Omega^{-\alpha_0})$, which, the reader should recall, leads to Eq. (A10), the components of the covariance matrix, q_2 , must satisfy $q_{2,kl} = \Omega^{-\alpha_k} S_{kl} + o(\Omega^{-\alpha_0})$ which, in turn, leads to $M_{1,k}(v, t) = 2 \sum_l v_l S_{2,kl}$. Note that whereas q_2 is a symmetric matrix, in general,

$\mathbf{S} = (S_{jk})$ is not. However, its components must satisfy $\Omega^{-\alpha_k} S_{kj} = \Omega^{-\alpha_j} S_{jk}$. Thus, Eq. (A13) reads:

$$\frac{dS_{jk}}{d\tau} = \frac{\Omega^{\alpha_1 - \alpha_k}}{(2\pi)^d} \sum_i \int_{-\infty}^{\infty} \left(2 \sum_l (r_{i,j} S_{kl} v_l + r_{i,k} S_{jl} v_l) + r_{i,j} r_{i,k} \right) e^{q(-v,\tau)} v_i(v) dv. \quad (\text{A14})$$

Finally, to leading order, $q(-v, t) = -i v \cdot s + o(\Omega^{-\alpha_0})$, so that Eq. (A9):

$$\frac{1}{\Omega^{\alpha_1 - \alpha_j}} \frac{ds_j}{d\tau} = \sum_i r_{i,j} v_i(s) \text{ if } j \neq j_1, \quad (\text{A15})$$

$$\frac{ds_{j_1}}{d\tau} = \sum_i r_{i,j_1} v_i(s) \text{ if } j = j_1, \quad (\text{A16})$$

and, as for Eq. (A14),

$$\begin{aligned} \frac{1}{\Omega^{\alpha_1 - \alpha_k}} \frac{dS_{jk}}{d\tau} = & \sum_i 2 \sum_l \left(r_{i,j} S_{kl} \frac{\partial v_i(s)}{\partial s_l} + r_{i,k} S_{jl} \frac{\partial v_i(s)}{\partial s_l} \right) \\ & + \sum_i r_{i,j} r_{i,k} v_i(s) \text{ if } j \neq j_1, \end{aligned} \quad (\text{A17})$$

$$\begin{aligned} \frac{dS_{jj_1}}{d\tau} = & \sum_i 2 \sum_l \left(r_{i,j} S_{j_1 l} \frac{\partial v_i(s)}{\partial s_l} + r_{i,j_1} S_{jl} \frac{\partial v_i(s)}{\partial s_l} \right) \\ & + \sum_i r_{i,j} r_{i,j_1} v_i(s) \text{ if } j = j_1, \end{aligned} \quad (\text{A18})$$

with $\Omega^{-\alpha_k} S_{kj} = \Omega^{-\alpha_j} S_{jk}$. Finally, since $\alpha_j < \alpha_1$ for all $j \neq j_1$, the quasi-steady state approximation can be applied to Eqs. (A15) and (A17), thus leading to Eqs. (8) and (9)

$$\begin{aligned} \Omega^{-\frac{2\alpha_1 - \alpha_j - \alpha_k}{2}} \frac{dS_{jk}}{d\tau} &= \frac{1}{(2\pi)^d} \sum_i \int_{-\infty}^{\infty} \left(i \sum_n (v_n S_{nj} r_{i,k} + v_n S_{nk} r_{i,j}) + r_{i,j} r_{i,k} \right) e^{q(-v,\tau)} v_i(v) dv \text{ if } j \neq k, \\ \Omega^{-\alpha_1 + \alpha_j} \frac{dS_{jj}}{d\tau} &= \frac{1}{(2\pi)^d} \sum_i \int_{-\infty}^{\infty} \left(2i \sum_n v_n S_{nk} r_{i,j} + r_{i,j}^2 \right) e^{q(-v,\tau)} v_i(v) dv \text{ if } j \neq j_1, \\ \frac{dS_{jj}}{d\tau} &= \frac{1}{(2\pi)^d} \sum_i \int_{-\infty}^{\infty} \left(2i \sum_n v_n S_{nj}(v, \tau) r_{i,j} + r_{i,j}^2 \right) e^{q(-v,\tau)} v_i(v) dv \text{ if } j = j_1, \end{aligned} \quad (\text{A19})$$

where the matrix \mathbf{S} is such that $\mathbf{S} = (S_{jk})$.

This almost completes our derivation of the evolution equations for the lowest order approximation for the first and second cumulant since the scaling substitutions for $q_n(t)$ emerging from Eq. (A1) imply that:^{11,29}

$$q(u, t) = \rho(\epsilon, u, t), \quad (\text{A20})$$

where

$$\rho(\epsilon, u, t) = i u \cdot q_1 - \frac{1}{2} \sum_{j,i} \Omega^{-(\alpha_j + \alpha_k)/2} u_j u_k S_{jk} + o(\Omega^{-\alpha_1}). \quad (\text{A21})$$

Therefore, to leading order, $e^{q(-v,t)} \simeq e^{-i v \cdot q_1}$, which means that, after inverting the corresponding Fourier transforms, Eqs. (A9) and (A19) can be written as

$$\begin{aligned} \frac{1}{\Omega^{\alpha_1 - \alpha_j}} \frac{dq_{1,j}}{d\tau} &= \sum_i r_{i,j} v_i(q_1) \text{ if } j \neq j_1, \\ \frac{dq_{1,j_1}}{d\tau} &= \sum_i r_{i,j_1} v_i(q_1), \end{aligned} \quad (\text{A22})$$

and

$$\begin{aligned}\Omega^{-\frac{2\alpha_1-\alpha_j-\alpha_k}{2}} \frac{dS_{jk}}{d\tau} &= \sum_i \left(\sum_n S_{nj} r_{i,k} \frac{\partial v_i(q_1)}{\partial q_{1,n}} + r_{i,j} \frac{\partial v_i(q_1)}{\partial q_{1,n}} S_{nk} \right) + r_{i,j} r_{i,k} v_i(q_1) \text{ if } j \neq k, \\ \Omega^{-\alpha_1+\alpha_j} \frac{dS_{jj}}{d\tau} &= \sum_i \left(\sum_n S_{nj} r_{i,j} \frac{\partial v_i(q_1)}{\partial q_{1,n}} + r_{i,j} \frac{\partial v_i(q_1)}{\partial q_{1,n}} S_{nj} \right) + r_{i,j}^2 v_i(q_1) \text{ if } j \neq j_1, \\ \frac{dS_{jj}}{d\tau} &= \sum_i \left(\sum_n S_{nj} r_{i,j} \frac{\partial v_i(q_1)}{\partial q_{1,n}} + r_{i,j} \frac{\partial v_i(q_1)}{\partial q_{1,n}} S_{nj} \right) + r_{i,j}^2 v_i(q_1) \text{ if } j = j_1.\end{aligned}\quad (\text{A23})$$

We can now apply the quasi-steady state approximation to Eqs. (A22) and (A23), i.e., by setting $\frac{\Omega^{\alpha_j}}{\Omega^{\alpha_1}} \frac{dq_{1,j}}{d\tau} = 0$ and $\Omega^{-\frac{2\alpha_1-\alpha_j-\alpha_k}{2}} \frac{dS_{jk}}{d\tau} = 0$ and $\Omega^{-\alpha_1+\alpha_j} \frac{dS_{jj}}{d\tau} = 0$, we obtain Eqs. (8) and (9).

Note that, although we have computed here the lowest order approximations for the first and second cumulants (i.e., mean value and covariance matrix, respectively), this asymptotic method can be extended to higher-order cumulants to go beyond the Gaussian approximation.^{11,29}

APPENDIX B: HJQSS APPROXIMATION FOR THE BISTABLE STOCHASTIC TYSON-NOVAK SYSTEM

In this appendix, we derive the HJQSS approximation for the Tyson and Novak system, Eqs. (56)–(62). The Hamilton equations (Eqs. (24) and (25)) corresponding to the rescaled Hamiltonian equation (55) are given by

$$\begin{aligned}\frac{dx_1}{d\tau} &= p_7 x_7 (-p_3 x_1 x_3 + \kappa_2 p_3 x_5) \\ &\quad + \kappa_6 p_4 x_6 + \kappa_8 \alpha (1 - p_7) x_1 x_7,\end{aligned}\quad (\text{B1})$$

$$\frac{dx_2}{d\tau} = \kappa_3 p_7 p_3 x_5 x_7 - \kappa_4 p_4 x_2 x_4 + \kappa_5 p_4 x_6, \quad (\text{B2})$$

$$\epsilon \frac{dx_3}{d\tau} = p_7 x_7 (-p_1 x_1 x_3 + \kappa_2 p_1 x_5 + \kappa_3 p_2 x_5), \quad (\text{B3})$$

$$\epsilon \frac{dx_4}{d\tau} = -\kappa_4 p_2 x_2 x_4 + \kappa_5 p_2 x_6 + \kappa_6 p_1 x_6, \quad (\text{B4})$$

$$\epsilon \frac{dx_5}{d\tau} = p_7 x_7 (x_1 x_3 - \kappa_2 x_5 - \kappa_3 x_5), \quad (\text{B5})$$

$$\epsilon \frac{dx_6}{d\tau} = \kappa_4 x_2 x_4 - \kappa_5 x_6 - \kappa_6 x_6, \quad (\text{B6})$$

$$\frac{dx_7}{d\tau} = \kappa_7 - \kappa_8 (1 + \alpha p_1 x_1) x_7, \quad (\text{B7})$$

and

$$\frac{dp_1}{d\tau} = -p_7 x_7 (p_5 - p_1 p_3) x_3 - \kappa_8 \alpha (1 - p_7) x_7, \quad (\text{B8})$$

$$\frac{dp_2}{d\tau} = -\kappa_4 (p_6 - p_2 p_4) x_4, \quad (\text{B9})$$

$$\epsilon \frac{dp_3}{d\tau} = -p_7 x_7 (p_5 - p_1 p_3) x_1, \quad (\text{B10})$$

$$\epsilon \frac{dp_4}{d\tau} = -\kappa_4 (p_6 - p_2 p_4) x_2, \quad (\text{B11})$$

$$\epsilon \frac{dp_5}{d\tau} = -p_7 x_7 (\kappa_2 (p_1 p_3 - p_5) + \kappa_3 (p_2 p_3 - p_5)), \quad (\text{B12})$$

$$\epsilon \frac{dp_6}{d\tau} = -\kappa_5 (p_2 p_4 - p_6) - \kappa_6 (p_1 p_4 - p_6), \quad (\text{B13})$$

$$\begin{aligned}\frac{dp_7}{d\tau} &= -p_7 (\kappa_2 (p_1 p_3 - p_5) + \kappa_3 (p_2 p_4 - p_5)) x_5 \\ &\quad - (1 - p_7) \kappa_8 (1 + \alpha p_1 x_1),\end{aligned}\quad (\text{B14})$$

where $\epsilon = e_0/s_0$. For simplicity, we have dropped the hats in the notation for the rescaled x -variables. We can now apply the quasi-steady state approximation to these equations, namely, $\epsilon \frac{dx_i}{d\tau} = 0$ and $\epsilon \frac{dp_i}{d\tau} = 0$, $i = 3, \dots, 6$:

$$\begin{aligned}\frac{dx_1}{d\tau} &= p_7 x_7 (-p_3 x_1 x_3 + \kappa_2 p_3 x_5) + \kappa_6 p_4 x_6 \\ &\quad + \kappa_8 \alpha (1 - p_7) x_1 x_7,\end{aligned}\quad (\text{B15})$$

$$\frac{dx_2}{d\tau} = \kappa_3 p_7 p_3 x_5 x_7 - \kappa_4 p_4 x_2 x_4 + \kappa_5 p_4 x_6, \quad (\text{B16})$$

$$-p_1 x_1 x_3 + \kappa_2 p_1 x_5 + \kappa_3 p_2 x_5 = 0, \quad (\text{B17})$$

$$-\kappa_4 p_2 x_2 x_4 + \kappa_5 p_2 x_6 + \kappa_6 p_1 x_6 = 0, \quad (\text{B18})$$

$$x_1 x_3 - \kappa_2 x_5 - \kappa_3 x_5 = 0, \quad (\text{B19})$$

$$\kappa_4 x_2 x_4 - \kappa_5 x_6 - \kappa_6 x_6 = 0, \quad (\text{B20})$$

$$\frac{dx_7}{d\tau} = \kappa_7 - \kappa_8 (1 + \alpha p_1 x_1) x_7, \quad (\text{B21})$$

and

$$\frac{dp_1}{d\tau} = -p_7 x_7 (p_5 - p_1 p_3) x_3 - \kappa_8 \alpha (1 - p_7) x_7, \quad (\text{B22})$$

$$\frac{dp_2}{d\tau} = -\kappa_4 (p_6 - p_2 p_4) x_4, \quad (\text{B23})$$

$$p_5 - p_1 p_3 = 0, \quad (\text{B24})$$

$$p_6 - p_2 p_4 = 0, \quad (\text{B25})$$

$$\kappa_2(p_1 p_3 - p_5) + \kappa_3(p_2 p_3 - p_5) = 0, \quad (\text{B26})$$

$$\kappa_5(p_2 p_4 - p_6) + \kappa_6(p_1 p_4 - p_6) = 0, \quad (\text{B27})$$

$$\begin{aligned} \frac{dp_7}{d\tau} = & -p_7(\kappa_2(p_1 p_3 - p_5) + \kappa_3(p_2 p_4 - p_5))x_5 \\ & -(1 - p_7)\kappa_8(1 + \alpha p_1 x_1). \end{aligned} \quad (\text{B28})$$

Equations (B19) and (B20) together with the conservation laws $x_3 + x_5 = 1$ and $x_4 + x_6 = 1$ lead to

$$x_5 = \frac{x_1}{x_1 + (\kappa_2 + \kappa_3)}, \quad (\text{B29})$$

$$x_6 = \frac{x_2}{x_2 + \kappa_4^{-1}(\kappa_5 + \kappa_6)}. \quad (\text{B30})$$

Using Eqs. (B29) and (B30) in Eqs. (B15) and (B16), we obtain:

$$\frac{dx_1}{d\tau} = p_4 \frac{\kappa_4 x_2}{x_2 + J_2} - p_7 p_3 \frac{\kappa_3 x_7 x_1}{x_1 + J_1} + \kappa_8 \alpha (1 - p_7) x_7 x_1, \quad (\text{B31})$$

$$\frac{dx_2}{d\tau} = -p_4 \frac{\kappa_4 x_2}{x_2 + J_2} + p_7 p_3 \frac{\kappa_3 x_7 x_1}{x_1 + J_1}. \quad (\text{B32})$$

Furthermore, Eqs. (B24)–(B27) reduce to

$$p_5 - p_1 p_3 = 0, \quad (\text{B33})$$

$$p_6 - p_2 p_4 = 0, \quad (\text{B34})$$

$$p_2 p_3 - p_5 = 0, \quad (\text{B35})$$

$$p_1 p_4 - p_6 = 0. \quad (\text{B36})$$

Equations (B33)–(B36) imply that $p_1 = p_2$ and

$$\frac{dp_7}{d\tau} = -(1 - p_7)\kappa_8(1 + \alpha p_1 x_1). \quad (\text{B37})$$

Additionally, Eqs. (B33)–(B36), within the quasi-steady state approximation, imply that $H_A = H_B = 0$, and therefore the QSS Hamiltonian, H_{QSS} , is given by

$$H_{QSS}(x_7, p_7) = (1 - p_7)(-k_7 + k_8(1 + \alpha p_1 x_1)x_7). \quad (\text{B38})$$

Since the dynamics of the stochastic trajectories is confined to a manifold of constant energy, in particular to the $H = 0$ manifold, we must have that $H_{QSS} = 0$, so that:

$$p_1 = \frac{\kappa_7 - \kappa_8 x_7}{\kappa_8 \alpha x_1 x_7}, \quad (\text{B39})$$

with $p_1 = p_2$, and $p_3 = \frac{p_5}{p_1}$ and $p_4 = \frac{p_6}{p_1}$. These results, together with Eqs. (B21), (B31), (B32) and (B37) lead to the HJQSS approximation, Eqs. (56)–(62).

Equations (56)–(62) also provide us with the relation between the parameters of the Tyson and Novak model, Eq. (50), and those of the stochastic, Table III.⁴³

$$\kappa_2 = J_4 - \kappa_3,$$

$$\kappa_3 = \frac{a_4 m}{k_1 e_0 y_0},$$

TABLE V. Parameter values used in simulations of the stochastic Tyson and Novak system and numerical solution of the corresponding HJQSS.

Parameter	Units	Reference
$a'_1 = 0.04$	min^{-1}	40
$a'_2 = 0.04$	min^{-1}	40
$a''_2 = 1$	min^{-1}	40
$a_3 = 1$	min^{-1}	40
$a_4 = 35$	min^{-1}	40
$m = 0.4$	min^{-1}	...
$e_0 = 4$	Dimensionless	...
$s_0 = 400$	Dimensionless	...
$y_0 = 400$	Dimensionless	...
$k_1 = 1$	min^{-1}	13
$\kappa_6 = \kappa_3$	Dimensionless	...

$$\kappa_4 = \frac{a'_3}{k_1 e_0 y_0},$$

$$\kappa_5 = \kappa_4 J_1 - \kappa_6,$$

$$\kappa_7 = \frac{a'_1}{k_1 e_0 y_0},$$

$$\kappa_8 = \frac{a'_2}{k_1 e_0 y_0},$$

$$a = \frac{a''_2}{k_1 e_0 y_0 \kappa_8}.$$

The parameter values used in our simulations are given in Table V.

- ¹J. Keener and J. Sneyd, *Mathematical Physiology* (Springer-Verlag, New York, NY, USA, 1998).
- ²L. Michaelis and M. L. Menten, *Biochem. Z.* **49**, 333 (1913).
- ³G. E. Briggs and J. B. S. Haldane, *Biochem. J.* **19**, 338 (1925).
- ⁴S. Schnell and T. E. Turner, *Prog. Biophys. Mol. Biol.* **85**, 235 (2004).
- ⁵R. Grima and S. Schnell, *Biophys. Chem.* **124**, 1 (2006).
- ⁶H. Qian and E. L. Nelson, *Biophys. Chem.* **101–102**, 565 (2002).
- ⁷R. Grima, *Phys. Rev. Lett.* **102**, 218103 (2009).
- ⁸P. Thomas, A. V. Straube, and R. Grima, *J. Chem. Phys.* **135**, 181103 (2011).
- ⁹H. Berry, *Biophys. J.* **83**, 1891 (2002).
- ¹⁰N. G. van Kampen, *Stochastic Processes in Physics and Chemistry* (Elsevier, The Netherlands, 2007).
- ¹¹R. Kubo, K. Matsuo, and K. Kitahara, *J. Stat. Phys.* **9**, 51 (1973).
- ¹²H. Touchette, *Phys. Rep.* **478**, 1 (2009).
- ¹³C. V. Rao and A. P. Arkin, *J. Chem. Phys.* **118**, 4999 (2003).
- ¹⁴T. E. Turner, S. Schnell, and K. Burrage, *Comput. Biol. Chem.* **28**, 165 (2004).
- ¹⁵P. Thomas, A. V. Straube, and R. Grima, *J. Chem. Phys.* **133**, 195101 (2010).
- ¹⁶É. Dóka and G. Lente, *J. Chem. Phys.* **136**, 054111 (2012).
- ¹⁷P. Thomas, R. Grima, and A. V. Straube, *Phys. Rev. E* **86**, 041110 (2012).
- ¹⁸K. Burrage, T. Tian, and P. Burrage, *Prog. Biophys. Mol. Biol.* **85**, 217 (2004).
- ¹⁹D. G. Vlachos, *Adv. Chem. Eng.* **30**, 1 (2005).
- ²⁰S. MacNamara, K. Burrage, and R. B. Sidje, *Multiscale Model. Simul.* **6**, 1146 (2008).
- ²¹Y. Cao, D. T. Gillespie, and L. R. Petzold, *J. Comput. Phys.* **206**, 395 (2005).
- ²²Y. Cao, D. T. Gillespie, and L. R. Petzold, *J. Chem. Phys.* **122**, 014116 (2005).
- ²³A. Samant and D. G. Vlachos, *J. Chem. Phys.* **123**, 144114 (2005).
- ²⁴W. E, D. Liu, and E. Vanden-Eijnden, *J. Comput. Phys.* **221**, 158 (2007).
- ²⁵K. R. Sanft, D. T. Gillespie, and L. R. Petzold, *IET Syst. Biol.* **5**, 58 (2011).

- ²⁶M. Rathinam, L. R. Petzold, Y. Cao, and D. T. Gillespie, *J. Chem. Phys.* **119**, 12784 (2013).
- ²⁷E. L. Haseltine and J. B. Rawlings, *J. Chem. Phys.* **117**, 6959 (2002).
- ²⁸H. Salis and Y. Kaznessis, *J. Chem. Phys.* **122**, 054103 (2005).
- ²⁹T. Alarcón and K. M. Page, *J. R. Soc., Interface* **4**, 283 (2007).
- ³⁰V. Elgart and A. Kamenev, *Phys. Rev. E* **70**, 041106 (2004).
- ³¹K. Ball, T. G. Kurtz, L. Popovic, and G. Rempala, *Ann. Appl. Probab.* **16**, 1925 (2006).
- ³²M. Assaf, B. Meerson, and P. V. Sasorov, *J. Stat. Mech.: Theory Exp.* P07018 (2010).
- ³³D. T. Gillespie, *J. Comput. Phys.* **22**, 403 (1976).
- ³⁴M. I. Dykman, T. Horita, and J. Ross, *J. Chem. Phys.* **103**, 966 (1995).
- ³⁵R. Dickman and R. Vidigal, *Braz. J. Phys.* **33**, 73 (2003).
- ³⁶U. C. Täuber, M. Howard, and B. P. Vollmayr-Lee, *J. Phys. A: Math. Gen.* **38**, R79 (2005).
- ³⁷R. P. Feynman and A. R. Hibbs, *Quantum Mechanics and Path Integrals* (Dover Publications, Mineola, NY, USA, 2010).
- ³⁸J. D. Murray, *Asymptotic Analysis* (Springer-Verlag, New York, NY, USA, 1984).
- ³⁹M. J. Ablowitz and A. S. Fokas, *Complex Variables: Introduction and Applications* (Cambridge University Press, Cambridge, UK, 2003).
- ⁴⁰J. J. Tyson and B. Novak, *J. Theor. Biol.* **210**, 249 (2001).
- ⁴¹D. Liu, *J. Chem. Phys.* **124**, 164104 (2006).
- ⁴²D. Liu, *J. Comput. Phys.* **227**, 8672 (2008).
- ⁴³P. Guerrero and T. Alarcón, “Stochastic multiscale models of cell population dynamics: Asymptotic and numerical methods,” *Math. Model. Nat.* (submitted).
- ⁴⁴P. G. Bolhuis, D. Chandler, C. Dellago, and P. L. Geissler, *Annu. Rev. Phys. Chem.* **53**, 291 (2002).
- ⁴⁵E. Vanden-Eijnden, *Lect. Notes Phys.* **703**, 453 (2006).
- ⁴⁶W. E and E. Vanden-Eijnden, *Annu. Rev. Phys. Chem.* **61**, 391 (2010).